Bioengineering of a Novel Peptide Sequence from the Venom of *Conus obscurus*

A THESIS TO THE GRADUATE DIVISION OF THE UNIVERSITY OF HAWAIʻI AT MĀNOA IN FULL FULFILLMENT OF THE REQUIREMENTS FOR THE DEGREE OF

MASTER OF SCIENCE

IN

MOLECULAR BIOSCIENCES AND BIOENGINEERING

December 2021

By

Sean C. Wiere

Thesis Committee:

Jon-Paul Bingham (Chairperson)
Daniel Owens
Qing X. Li

Acknowledgments

I am indebted towards my good friend and mentor, Dr. Jon-Paul Bingham for taking me in and showing me the way to becoming a better student, person, and scientist.

I am grateful for all the help from the good friends I have made in the Bingham Laboratory, including Erick Delgado, Nicholas Sinclair, Angelica Valdez, Dr. Rui-Yang Zhang, Brandon Day, Bridget Murphy, Vincent Paul Aurelio, Chloe Delos Reyes, Dr. Dawson Fogen, Nicole Yuzon, and Amihan Camson. They always included me even if I couldn't make it to many lab parties due to COVID.

I am thankful for the support from Dr. Daniel Owens and Dr. Qing X Li and the great talks I have had with them over the years.

I appreciate the functional characterization data from Dr. Steven Peigner and Dr. Jan Tytgat at the Laboratory of Toxicology at the University of Leuven, MS data from Dr. Randy Wittal at the Department of Chemistry of the University of Alberta, and amino acid analysis data from the Molecular Structure Facility of the University of California, Davis. Without the data from the scientists above, this thesis would not be possible.

I am thankful for the funding from the Graduate Student Organization and the Giving Tree Scholarship and the guidance from the Department of Molecular Biosciences and Bioengineering staff at the University of Hawai‘i, Mānoa.

Last but not least, I would like to give my endless thanks to the continual support of my loving wife and family.

Abstract

The marine cone snail produces one of the fastest prey strikes in the animal kingdom with efficacious venom injection causing prey paralysis and death within seconds. Each snail produces hundreds of conotoxins and has been the source behind discovering and utilizing novel analgesic peptide therapeutics. In this study, we discover, isolate, and synthesize two α3/5 conotoxins derived from the milked venom of *Conus obscurus*: one novel (α-conotoxin ObI) and one previously found in the venom of *Conus striatus* (α-SI). We then generate five synthetic analogs, accompanying single and double mutations from the native α-conotoxin ObI. We integrate three post-translational modifications (PTMs) within analog development: *N*-terminal truncation, proline hydroxylation, and tryptophan bromination. α-Conotoxin ObI demonstrates nanomolar potency towards *Poecilia reticulata* (LD_{50}) and the *Homo sapiens* muscle-type nAChR (EC_{50}). Moreover, the analog α-ObI [P9K] displayed enhanced potency in both animal bioassays. The exhibited successful incorporation of 3 PTMs investigates the boundaries of peptide bioengineering in the generation of novel α-conotoxins.

Table of Contents

Figures

Tables

Abbreviations

Abbreviation	Description
α	Alpha
αα	Amino acid
αA	Alpha conotoxin superfamily
αβδ	Delta muscle nAChR subunit
αβγ	Gamma muscle nAChR subunit
αβδγ	Fetal muscle nAChR subunit
αβδϵ	Adult muscle nAChR subunit
β	Beta
δ	Delta
ϵ	Epsilon
γ	Gamma
μ	Mu
ω/Ω	Omega
°C	Celsius
*	*C*-terminal amidation
M	Molar
mM	Millimolar
μM	Micromolar
nM	Nanomolar
$[MH]^+$	Monoisotopic mass
ACE	Angiotensin-converting enzyme
ACh	Acetylcholine
acm	Acetamidomethyl
ANOVA	Analysis of variance
Aq.	Aqueous
BC_3H-1	Mouse cell

BLAST	Basic local alignment search tool
Br^-	Bromine
$CaCl_2$	Calcium dichloride
Ca_v	Voltage-gated calcium
cDNA	Complementary DNA
CID	Collision-induced dissociation
CNS	Central nervous system
cRNA	Complementary RNA
Ctx	Conotoxin
D	Dose
Da	Dalton
DCM	Dichloromethane
DI	De-Ionized
DIEA	N,N-Diisopropylethylamine
DMF	Dimethylformamide
EC_{50}	Half maximal effective concentration
EDT	Electron transfer dissociation
ESI	Electrospray ionization
FDA	Food and drug administration
fmoc-SPPS	9-Fluorenylmethoxycarbonyl solid-phase peptide synthesis
HCL	Hydrochloride
Hyp	Hydroxyproline
IC_{50}	Half maximal inhibitory concentration
ICK	Inhibitor cysteine knot
KCl	Potassium chloride
K_v	Voltage-gated potassium
LD_{50}	Median lethal dose
m/v	Mass-to-volume
m/z	Mass-to-charge
MALDI	Matrix-assisted laser desorption ionization
MeCN	Acetonitrile

$MgCl_2$	Magnesium chloride
mRNA	Messenger RNA
MS	Mass spectrometry
MV	Milked Venom
N_2	Dinitrogen
$Na_2S_2O_3$	Sodium thiosulfate
nAChR	Nicotinic acetylcholine channel receptor
NaCl	Sodium chloride
Na_v	Voltage-gated sodium
NH_4HCO_3	Ammonium bicarbonate
NMR	Nuclear magnetic resonance
PBS	Phosphate buffered saline
PDA	Photodiode array
pH	Potential hydrogen
PTM	Post-translational modification
Ref.	Reference
RMSD	Root-mean-square deviation
RP-HPLC	Reversed-phase high-performance liquid chromatography
SAR	Structure-activity relationship
SEM	Mean ± standard error
Solvent A	0.1% TFA in *aq.* (v/v)
Solvent B	90% MeCN, 0.08% TFA in *aq.* (v/v)
T	Time
TFA	Trifluoroacetic acid
TOF	Time-of-flight
t_R	Retention time
trt	Trityl
UV	Ultraviolet
v/v	Volume-to-volume
w/v	Weight of solution

Chapter 1: Introduction

1.1 The History of Peptide Research

1.1.1 Peptide Drug production in Big Pharma

The use of peptides for medicinal purposes has boomed over the past 100 years. The pioneer of these therapeutic compounds started during World War I with opiate morphine and cyclic peptide penicillin, followed by the commercialization and production of insulin in the early 1920s. Ever since then, peptide drugs have significantly reshaped our modern pharmaceutical history. More recently, over the past two decades, more than 30 peptide pharmaceuticals have been FDA approved, with over 60 in total worldwide ([1]). Although some problems arise with peptide drugs, the beneficial characteristics of peptides can match the popularity of small molecule drugs. Peptides, peptide fragments, and αα's control and coordinate most human physiological processes. Thus, they are considered naturally occurring biologics and have higher efficacy and safety standards than synthetic drugs ([2]). Other benefits of peptide drugs include shorter half-life leading to less accumulation in the body (reduces the risk of exposure to degradation products), ability to penetrate deeper into the tissue, less immunogenic, lower manufacturing costs, higher activity, and excellent stability (can be stored at room temperature) ([2]).

The current age of the pharmaceutical industry is experiencing some dramatic changes, including increased safety regulations, lengthy compound development processes, and massive financial efforts ([3]). There has been an increase in investments for research and development, but at the same time a decrease in medical innovation. Orphan or repurposed drugs reduce production costs compared to expensive drug development, leading to fewer new drugs ([4]). Uhlig *et al.* ([4]) and Vleighe *et al.* ([3]) agree that new strategies are needed to revive the lost momentum of the drug production industry, and they believe that solution starts with peptides. The utilization of peptides as therapeutics has evolved and will continue to evolve with new drug development and treatment methods ([5]).

1.1.2 The Age of Venomous Peptides

Usage of venom by humans goes all the way to ancient times when warriors dip the tip of their spears in venom as a secondary weapon. Later on, venoms from snakes, toads, and spiders were used as traditional remedies for treating prevalent human ailments like arthritis and cancers ([6]). The earliest known use of venom goes back to 37 B.C.E. as the Roman historian Appian describes a Scythian doctor administering a small amount of steppe viper venom onto a wound to stop the profuse bleeding and save the man's life ([7]). Until the late 20th century, these venoms from many animals were recognized as treasure troves for bioactive peptides. Captopril, an inhibitor of angiotensin-converting enzyme (ACE), was isolated from *Bothrops jararaca* snake venom was discovered in 1981 ([8]). From there, venom from many species, including snakes, scorpions, and cone snails, led the interest in producing FDA-approved peptide drugs for many diseases including pain, drug addiction, and central nervous system (CNS) disorders.

A variety of venoms are found in nearly all of the phyla throughout the animal kingdom; Cnidaria (jellyfish), Arthropoda (spiders, ants, and centipedes), Mollusca (cone snails and octopuses), and Chordata (reptiles, fish, amphibians, and mammals) to name a few. These organisms have evolved to produce multiple enzymes, inorganic salts, low molecular weight organic compounds, neurotoxins, antimicrobial, and cytolytic peptides as a defense/predatory mechanism against predator/prey. The venom profile of a single species can contain up to thousands of different bioactive peptides, leaving the total pool of unique peptides reaching possibly greater than ten million ([9]). For example, hundreds of thousands of bioactive peptides can be found in the 700 different cone snail species alone ([10], [11], [12]). To add on top of that, other species extensively studied for their venom content include ~48,300 species of spiders, ~3,500 species of snakes ([13]), and ~2,000 species of scorpions ([14]).

There are many venomous peptides from different species that have seen clinical trial phase development and FDA approval. Table 1 shows the wide range of peptides sourced from animal venom that have been discontinued or are currently being used today. Isolation of these naturally produced products has developed leads into potential novel therapeutic agents for many human diseases and applications in cosmetics and agriculture. A 22-residue protein isolated from

the snake species *Tropidolaemus walgeri* called Walgerin-1 is a nicotinic acetylcholine channel receptor (nAChR) blocking peptide with a similar mechanism to botulinum toxin-A (BoTox^{TM}) ([15]). A neuromuscular $Na_v1.4$ blocking μ-conotoxin from the cone snail species *Conus consors* reduced fine line wrinkles by 80% for 12-18 hours after application in a 1% w/v topical cream ([6]). Agriculture applications for venomous peptides include a 37-residue disulfide-rich protein found in the venom of the Australian Blue Mountain funnel-web spider called ω-HXTX-Hv2a that was launched in 2017 by Venomix ([16]). This peptide acts as an insecticide and blocks insect voltage-gated calcium (Ca_v) channels, with 10,000-fold selectivity for insect Ca_v channels over vertebrate Ca_v channels ([6]). This peptide has high stability, showing resistance to hot summer conditions with no loss in bioactivity due to its inhibitor cysteine knot (ICK) ([17]).

Table 1: Pharmaceuticals originating from venom peptides that have reached clinical trial or FDA approval.

Animal	Drug Name	Action of Class	Species	Status	Year	Ref.
Snake	Captopril	ACE inhibitor	*Bothrops jararaca*	FDA approved	1981	[18]
	Eptifibatide	GPIIb/IIIa integrin receptor	*Sistrurus miliarius barbouri*	FDA approved	1998	[19]
	Tirofiban	GPIIb/IIIa integrin receptor	*Echis carinatus*	FDA approved	1999	[19]
	Ancrod	Cleave fibrinogen	*Calloselasma rhodostoma*	Phase 3	2009	[20]
	Cenderitide	DNP/CNP regulator	*Dendroaspis angusticeps*	Phase 2	2017	[6]
Sea Anemone	Dalazatide	K_v1.1, 1.3 channel blocker	*Stichodactyla helianthus*	Phase 1	Current	[21]
Lizard	Exenatide	GLP-1 receptor agonist	*Heloderma suspectum*	FDA approved	2005	[6]
Scorpion	TM601	Ca2+ chloride channel inhibitor	*Leiurus quinquestriatus*	Phase 3	2008	[22]
	Tozuleristide	Fluorescent peptide for surgery	*Leiurus quinquestriatus*	Phase 1	Current	[6]
Shrew	SOR-C_{13}	TRPV6 inhibitor	*Blarina brevicauda*	Phase 1	Current	[6]
Leech	Lepirudin	Thrombin inhibitor	*Hirudo medicinalis*	FDA approved	1998	[23]
	Bivalirudin	Thrombin inhibitor	*Hirudo medicinalis*	FDA approved	2000	[24]
Cone Snail	Ziconotide	Ca_v2.2 inhibitor	*Conus magus*	FDA approved	2004	[25]
	AM336 (CVID)	Ca_v2.2 inhibitor	*Conus catus*	Phase 2	2004	[26]
	ACV1	α9α10 nAChR inhibitor	*Conus victoriae*	Phase 2	2007	[6]
	Xen2174	norepinephrine transporter inhibitor	*Conus marmoreus*	Phase 2	2008	[27]
	Conantokin-G (CGX-1007)	NMDA receptors NR2B	*Conus geographus*	Phase 2	2011	[6]
	Conantokin-T (CGX-100)	NMDA receptor NR2A and NR2B	*Conus geographus*	Phase 2	2011	[28]
	Contulakin-G (CGX-1160)	Neurotensin receptor agonist	*Conus geographus*	Phase 1	2016	[29]

1.1.3 Technological Developments in Venom Research

The ability to recognize and distinguish peptides in venom has become available over the past century due to the increasing instrument availability and methods. Classical chromatography methods were replaced with high-performance liquid chromatography (HPLC) methods to recover pure samples and Edman degradation for sequencing in the 1980s ([1]). In the 1990s, three-dimensional solution structures became available to view thanks to the improvements of nuclear magnetic resonance (NMR) instrumentation. This allowed for more transparent results of peptide structure/diversity and structure-activity relationship (SAR) studies. Increased instrumentation quality has evolved access to modern spectrometers and isotopic labeling ([31]). These valuable technological improvements gave more significant insights into how each venom component acted on its potential target ([6]).

The study of venomics (global study of venom and venom glands) allows scientists to find all the characteristics of a venom profile using genomics, transcriptomics, proteomics, and bioinformatics ([32]). The advancement in these studies has exponentially increased the number of peptides available to discover. Improvements in DNA, RNA, and protein sequencing techniques, along with database and computing algorithms, have improved the discovery of novel peptides in venom ([6]). The multiple processes that are involved in peptide discovery in the venom of cone snails, for example, are represented in Figure 1. Although, the high yield of venom peptide sequence discovery is not matched by the speed at which their function is assayed due to the significant efforts needed to characterize a single toxin alone ([9]).

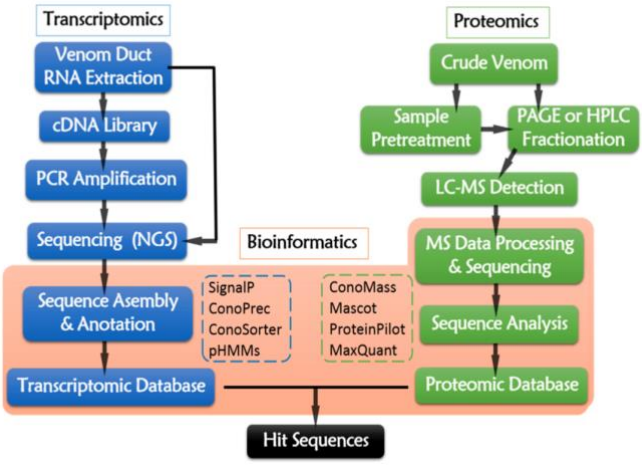

Figure 1: Diagram of the multi-process extraction for conotoxin discovery.

Figure gathered from Fu et al. ([33])

1.2 Enter *Conus*

1.2.1 Cone Snails and Conotoxins

The genus *Conus* (cone snails) is the world's largest genus of marine invertebrates ([34]). 700+ known species of *Conus* live in tropical to subtropical waters, such as the Indo-Pacific region, Australia and the Indian Ocean ([35]). Cone snails can be classified via three subgroups that are dependent on what they eat: piscivores (fish), molluscivores (mollusks), and vermivores (marine worms). However, some cone snail species are known to feed on more than one prey type ([36]).

Over millions of years, these slow-moving mollusks have evolved to develop a wide range of neuroactive, toxic peptides called conotoxins (with disulfide bonds) or conopeptides (without disulfide bonds). These peptides can cause paralysis, shudder, and even death of the prey within seconds of injection ([37]). The wide range of the *Conus* genus is estimated to produce up to 1,000,000 conotoxins ([33]) with a small conotoxin overlap in between species ([10]). Although, less than 1% of these bioactive peptides have been sequenced (~10,000), only a small percentage

of the 1% has been characterized pharmacologically ([38]). With that in mind, a single drop of this venomous cocktail can contain hundreds of bioactive conotoxins that can selectively modulate voltage and ligand-gated ion channels ([33]). Peptides from these carnivorous snails have provided a plentiful amount of research from the past six decades, ultimately leading to the discovery and development of a novel group of analgesic peptide therapeutics with ion specificity and isoform selectivity ([34]).

1.2.2 Cone Snail Venom Apparatus

Cone snails are very slow-moving creatures that have evolved a specialized envenomation apparatus for survival ([33]). The venom produced by the cone snail contains some of the most venomous neurotoxins globally. Still, the snail's prey strike is also considered one of the fastest in the animal kingdom, with peak acceleration strikes exceeding 400,000 m/s^2 ([39]). High acceleration of attack is due to a unique cellular latch mechanism within the snail to prevent advancement on the prey until sufficient pressure is achieved in the lumen of the proboscis ([40]). A hypodermic-like disposable tooth or radula (see Figure 2) is connected to the venom bulb via a tubular venom duct ([36]) and is hydraulically propelled out of the cone snails proboscis and harpooned deep into the dermal layers of their prey ([34], [39]). Effective prey capture entails a quick venom delivery system with fast-acting, neurotoxic conotoxins to overtake a prey's rapid escape response and cause almost instantaneous paralysis ([39]). To ensure a meal for the snail, venom is expelled through the tooth's lumen via the venom gland at the moment when the tooth is tethered into the prey.

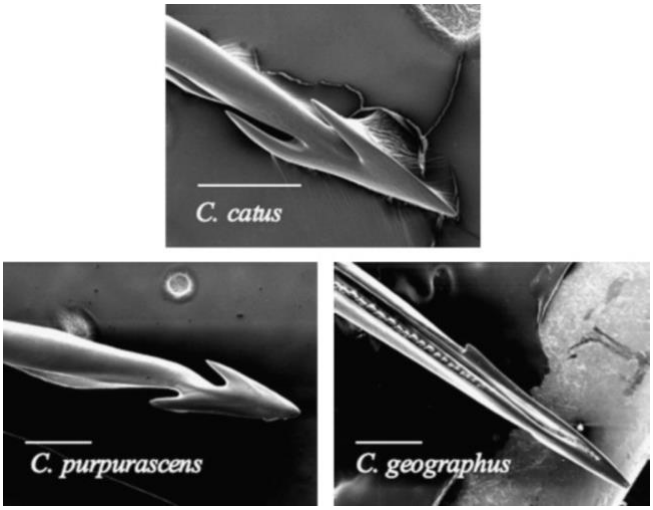

Figure 2: Radula from three different species of cone snail.

Characteristics of the radula can be used for the identification of species within Conus. Bingham et al. display three different cone snail harpoons via scanning electron micrographs at a 0.1 mm scale bar ([34]).

1.2.3 Feeding Behaviors of Cone Snails and Piscivore Introduction

Feeding behaviors can vary between the different subfamilies of *Conus* (piscivores, molluscivores, and vermivores). Molluscivores/vermivores impale and draw the mollusk/worm into their mouths with their harpoon-like radular. The feeding behavior and the characterization of piscivore relate to the focus of this thesis. Piscivore feeding behavior begins with Bingham *et al*. ([34]), tag and reel action, and netting. In the "tag and reel" harpooning method, the proboscis is extended and the radula impales, injects, and draws the fish into the fully expanded mouth or rostrum (as seen in molluscivores and vermivores) ([41], [34]). The second strategy called netting, as seen in *Conus geographus* and *Conus tulipa*, incorporates beating cilia-like projections on the mouth of the rostrum that stimulate the prey's side during engulfment ([34]). The calm beating of the cilia becomes chaotic once the engulfment process has been initiated, and the radula-like tooth harpoons the fish to begin envenomation once the rostrum is enclosed ([34]).

Piscivorous cone snails are the smallest subfamily within the *Conus* genus, representing ~7-10% of all the combined species ([34]). Though, the piscivores are the most dangerous and

contribute to several well-recorded human fatalities ([42]). The most dangerous species of cone snails that have caused the most deaths include *C. geographus* and *C. textile* ([43]). Although, other species have added to the fatalities, including *C. striatus* and *C. aulicus* ([44]). Most stings are due to specimen mishandling via scientists, divers, and shell collectors or simply by removing them from the marine environment ([34]). It is essential to mention that piscivore species have been extensively researched for their potential in therapeutic capabilities, so exposure to these dangerous species is high. It is also important to note that there is no antivenom for cone snail stings.

1.2.4 Conotoxin Classification and Function

Cone snail venom first attracted researchers during the 1960s to explain the many fatalities from cone snail stings ([36]). Shortly after, researchers estimated hundreds of thousands of neuroactive peptides (conopeptides) found in cone snail venom. Conopeptides can be classified into two groups; disulfide-poor peptides (contulakins, conantokins, conorfamides, conolysines, conophans, conomarphins, contryphans, conomap, and conopressins) and disulfide-rich peptides (conotoxins) ([36]). Conotoxins have been the main focus in research for their antinociceptive, antiepileptic, and cardio-/neuro-protective activity. They are valuable tools in research for many diseases ranging from Alzheimer's and cancer to drug addiction ([45])

Table 2: Conotoxin families and their corresponding mode of action.

Conotoxin Family	Mode of Action	Ref.
α	Inhibitory competitors of nicotinic acetylcholine receptors (nAChR)	46
γ	Acting on neuronal pacemaker currents affecting inward cation currents	47
δ	Acting on voltage-gated sodium (Na_v) channel VGSCs, activating and inactivating them	48
ε	Activating on G-protein-coupled presynaptic receptors or calcium channels	49
ι	Activating VGSCs	50
κ	Blocking voltage-gated potassium (K_v) channel VGKCs	51
μ	Blocking VGSCs	52
ρ	Inhibitors of alpha1-adrenoreceptors (GPRC)	53
σ	Acting on serotonin gated ion channels 5-HT3	54
τ	Acting on somatostatin receptors	55
χ	Inhibitors of neuronal noradrenaline transporters	53
ω	Acting on Ca_v channel VGCCs	56

Data gathered from Duque et al. ([57]).

Nomenclature is represented below. There is some variation in naming, but the overall conotoxin name is developed following a convention ([58]). The first Greek-letter indicates the conotoxin family represented in Table 2. The second two letters represent species name (*Conus consors*), followed by a roman numeral representing cysteine framework. Lastly, one uppercase letter indicating discovery order (A, B, C, etc.) ([36]):

α-CnIA

All conotoxins are translated from mRNA into prepropeptide precursors, consisting of a signal peptide region, a propeptide region, and a mature peptide region ([59]). There are many ways conotoxins can be classified. Conotoxin superfamilies' can be grouped based on similarities in nucleic acid sequences in the toxins signal peptide region ([60]). Though family classification overall can be represented based on the mode of action (refer to Table 2), regardless of their structural diversity and sequence similarities ([61]). Lastly, conotoxins can also be classified structurally based on their mature peptide sequence, as represented in Table 3.

The mature peptide sequence in conotoxins is highly diverse and can be categorized based on the locations of their cysteines, or cysteine framework, in the primary sequence (Table 3). These cysteine distribution patterns, pair connectivity, and the number of αα provide a peptide fold structure that favors their activity ([36], [57]). Other features that critically affect the conotoxin's bioactivity are the location of crucial αα residues within the sequence and post-translational modifications (PTMs). Multiple PTMs serve a specific purpose for prey paralysis, including *N*-terminal modifications, *C*-terminal modifications, intramolecular and intermolecular disulfide bonding, hydroxylation, γ-carboxylation, sulfation, bromination, *O*-glycosylation, and epimerization ([62]). These several PTMs have either a direct or speculative effect on bioactivity *in vivo* and may serve great importance in advancing proteomic screening ([62]). Further analysis of PTMs will be continued in Section 1.3 of this thesis.

Table 3: Cysteine frameworks with their corresponding cysteine pattern and family.

Framework	Cysteine Pattern	Disulfide bonds	Family
I	CC-C-C	2	α, ρ
II	CCC-C-C-C	3	α
III	CC-C-C-CC	3	α, ι, κ, μ
IV	CC-C-C-C-C	3	α, κ, μ
V	CC-CC	2	ε, μ, τ
VI/VII	C-C-CC-C-C	3	δ, γ, κ, μ, ω
VIII	C-C-C-C-C-C-C-C-C-C	5	α, σ
X	CC-CXOC	2	χ
XI	C-C-CC-CC-C-C	4	ι, κ
XIV	C-C-C-C	4	α, κ
XX	C-CC-C-CC-C-C-C-C	5	α
XXIV	C-CC-C	2	α
XXVI	C-C-C-C-CC-CC	4	ω
XXVIII	C-C-C-CCC-C-C	4	φ
XXVII	C-CC-C-C-C	3	δ, κ

X, any αα; O, hydroxyproline; Additional cysteine pattern frameworks not included in the table because the patterns have an undetermined pharmacological family. Data gathered from Jin et al. ([38]).

αα location within the primary mature peptide sequence is a significant part of developing synthetic analogs extensively in this thesis. Changing a single αα in a conotoxin sequence can change pharmacological activity from nanomolar to micromolar concentrations, or vice versa, due to a highly specific structure required to bind to a profoundly specific nAChR. Bioengineering these residues allow the scientist to develop unseen, novel synthetic analogs with high binding affinity and toxicity to the corresponding receptor.

1.2.5 Alpha Conotoxins

The alpha (α-) conotoxin family are among the first conotoxins to be discovered and are extensively researched for their pharmacological properties. The α-conotoxins, listing from 12-20 αα in length, generally act as competitive antagonists towards the nAChR and differentiate between several different subunits of the neuronal and the neuromuscular nAChR ([63]). The alpha conotoxin superfamily (αA), like the one we will be examining in this thesis, has a cysteine framework I of CC-C-C (see Table 3), represents ~75% of all the α-conotoxins ([58]), and has either/or neuromuscular and neuronal nAChR specificity. Although, α-conotoxins that have

nAChR specificity have been shown in nine different superfamilies; B, D, J, L, M, O1, S, T, and a yet unnamed family ([58]).

Within the αA-conotoxin superfamily, conotoxins display well-defined three-dimensional structures, predominantly due to the backbone connections of two disulfide bonds ([64]). These bonds form two disulfide loops that are represented as the *m* (loop 1) and *n* (loop 2). These conotoxins are then categorized into subfamilies based on the number of residues or αα in each loop between the cysteines (see Figure 3). αA-conotoxin subfamilies include 3/5, 4/3, 4/4, 4/5, 4/6, and 4/7. Conotoxins in the α3/5 subfamily are isolated from fish-hunting cone snails and block the neuromuscular nAChRs, while α-conotoxins 4/3, 4/4, 4/5, 4/6, 4/7 mainly interact with neuronal nAChRs ([64]). Conotoxins can also have varied structures due to the disulfide connections within the sequence. These structures include beaded, globular, and ribbon isomers (Figure 4). Several permutations can develop and generate new peptide isomers with distinct pharmacological and kinetic properties ([65]). As a result in most cases, disulfide bridges directly contribute to conotoxins' efficacy and biological variability ([62]).

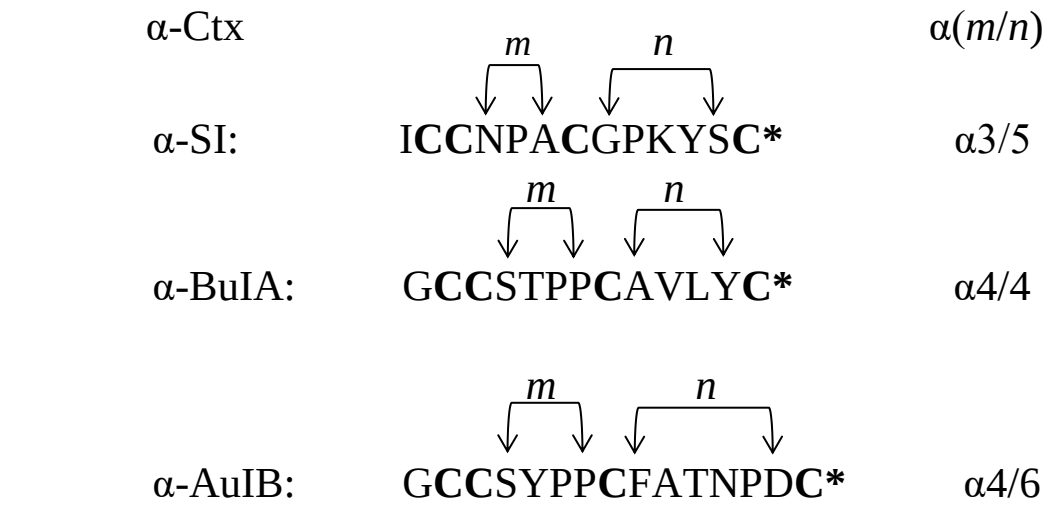

**, C-terminal amidation; Ctx, conotoxin*

Figure 3: α-Conotoxins with labeled *m* and *n* disulfide loops.

Their corresponding cysteine framework is listed to the right of the sequence.

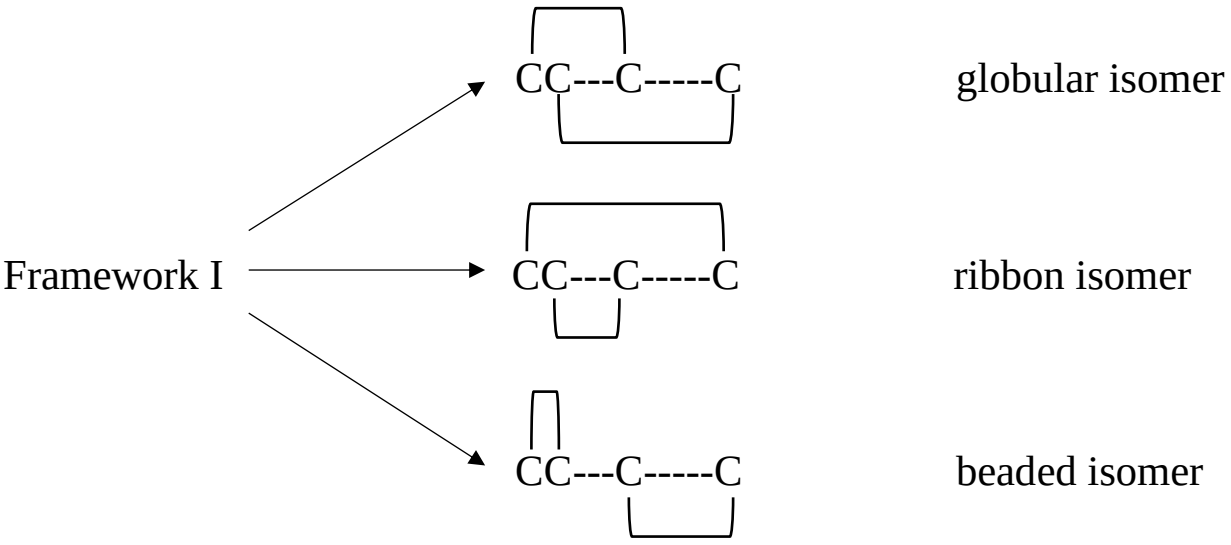

Figure 4: α-Conotoxin isomer structure.

The three different disulfide bond connections for α-conotoxins in cysteine framework I.

1.2.6 The nAChR and its Disease/Pharmaceutical Implications

At least one α-conopeptide has been discovered in each cone snail species, which supports the vital importance of the nAChR as a target ([58]). The nAChR is a ligand-gated cationic channel on the neuron that mediates fast synaptic transmission within the central and peripheral nervous systems ([66], [67], [64]). The nAChR can be found throughout many of species and serves as an essential platform for *in vivo* research in various animal models for human diseases ([64]).

In vertebrate species, there are two classes of nAChRs; neuromuscular and neuronal nAChRs. Respectively, both of these classes play crucial roles in neuromuscular and neurotransmission ([58]). Muscle-type nAChRs consist of four different subunits (α1β1ε/γδ) assembled in the order of α1γα1δβ1 ([68]). The fetal γ subunit is replaced with an ε subunit during maturity in amphibians and mammals. The neuronal nAChRs are much more complex in construction, consisting of homomeric and heteromeric combinations of α subunits (α2-α10) and β subunits (β2-β4) ([67], [69]). α-Conotoxins prefer binding to orthostatic sites between these subunits' interface on the nAChR ([64]). The many different neuronal subtypes of heteromeric combinations of α/β at other locations within the nervous system all play distinct pharmacological and biophysical roles ([67]).

1.3 Post-Translational Modifications and Mass Spectrometry Analysis

1.3.1 Post-Translational Modifications in Cone Snails

As said before, cone snails have evolved to produce some of the most toxic, fast-acting neurotoxins in the animal kingdom. *Conus* utilizes PTMs with preexisting modification enzymes recruited in the venom ducts to diversify venom constituents ([70]). PTMs are covalent modifications within αα that pertain to side chains or 'R' group functions ([62]). Once mRNA translation proceeds a polypeptide, or prepropeptide precursor, the *N*-terminal signal peptide and propeptide region are enzymatically cleaved, leaving behind a mature conopeptide at the *C*-terminal end. The mature region of the sequence is then subjected to a wide range of PTMs that

can change the overall three-dimensional structure of the peptide. This level of processing adds another layer of peptide diversity while increasing peptide effectiveness and stability. Each modification is known to serve a specific purpose to achieve the overall goal of prey immobilization.

Incorporating PTMs creates new challenges in proteomics and opens more opportunities to study structure-activity relationships, and ultimately increases the chance for further drug development. Current research creates and mimics the desired PTM *in vitro* through either chemical stimulation (oxidation) or the integration of chemically derived non-native αα during peptide synthesis. While using state-of-the-art analytical proteomic tools and a deep repertoire of modification methods, scientists can add PTMs synthetically to fine-tune conotoxin function.

1.3.2 Sequencing and Mass Spectrometry Techniques Involved in PTM Identification

Accuracy in conotoxin sequencing is a must. Although, some PTMs being analyzed today are exceedingly difficult to detect by the most advanced analytical methodologies. The increase of technological advancement in proteomics enhances the need to accurately predict when polypeptide products of genes are post-translationally modified ([70]). The case of incorrectly identifying a PTM in a conotoxin/conopeptide sequence could diminish the biological activity of that peptide.

Traditional methods of PTM discovery include cDNA characterization, αα analysis, Edman degradation and isotopic labeling ([71]). Although, these methods brought up some issues when it comes to PTM identification in *Conus* peptides. cDNA characterization was a great tool to sequence the King-Kong peptide in 1990 ([72]), a first using cDNA, and has been the mainstream identification method for many different conopeptides. However, cDNA characterization has shown limitations due to the inaccuracy of identifying PTMs from cDNA alone ([62]). Edman degradation coupled with αα composition analysis has been a staple for conotoxin sequencing and discovery. However, this method requires pure material and has limited ability to identify PTMs ([73]).

Current advancements in mass spectrometry analysis have been instrumental in identifying novel peptides as PTMs typically affect the molecular weight of the peptide, and this mass change can be detected. Mass spectrometry's advantages in identifying PTMs include: (i) high sensitivity with ranging intensities, (ii) ability to detect the location of PTM, (iii) unique fragmentation capabilities which lead to PTM identify confirmation, (iv) novel PTM discovery, compared to laborious biochemical techniques, (v) and the ability to identify PTMs in complex mixtures of proteins ([71],[73]). A coalition of traditional biochemical techniques, mass spectrometry and novel proteomic and genomic methodologies enables the discovery of most PTMs. Although, there are still issues to highlight as each PTM brings its challenge for identification.

Every PTM interpreted below is relevant to the specific conotoxins found in this research. The PTMs include; *C*-terminal amidation, disulfide bonding, *N*-terminal truncation, proline hydroxylation, and the bromination of tryptophan. Each modification will be explained in detail, along with its past effects on bioactivity. Each PTM will also include details on mass spectrometry identification and potential issues that can occur.

1.3.3 *C*-terminal Amidation and Disulfide Bonding

Two of the most abundant PTMs seen within the *Conus* genus are *C*-terminal amidation and disulfide bonding. The addition of a *C*-terminal amide is estimated to be found in about 127 conotoxins and can be seen throughout the *Conus* superfamilies ([74]). The *C*-terminal modification affects the overall isoelectric point and net charge state, which neutralizes the potential for deprotonation ([62]). *C*-terminal amidation is achieved through enzymatic cleavage of a *C*-terminal glycine at an *N*-*C* bond; while retaining the remains of the original peptide bond from the neighboring *C*-terminal αα ([75]). There are very few conotoxins with no disulfide bonds. Most conotoxins have a range of 1-3 disulfide bonds, with some conotoxins going as high as ten ([76]). Disulfide bonding allows for the formation of tertiary structures that are needed for peptide/receptor binding. This covalent bond is derived from two thiol groups that can interlink multiple pairs of cysteines, causing a disulfide framework. These bonds create different peptide isomers and αα loops that are paramount for receptor specificity ([76]).

Taking away the pre-PTM glycine in ω-conotoxin MVIIA gives scientists the chance to see what *C*-amidation does for conotoxin function. The analysis of ω-conotoxin MVIIA indicated a decreased folding efficiency without a pre-PTM glycine ([75]). *C*-terminal amidation is can also play a pivotal role in disulfide bond connectivity arrangement (isomer configuration), as shown in α-conotoxin ImI ([77]). Last, new research on α-conotoxin LsIA shows *C*-terminal amidation allows an increased number of contacts favored by binding to the α7 nAChR over *C*-terminal carboxylation ([78]).

The deletion of disulfide bonds can have various effects on conotoxin bioactivity. Substitution of alanine for cysteine in μ-conotoxin KIIIA, a deletion of one disulfide bridge, had comparable activity towards rat $Na_v1.2$ channels compared to the native form ([79]). Alternatively, the substitution of two serines for two cysteines in ω-conotoxin GVIA, a deletion of one disulfide bridge, resulted in an 8,000-fold loss in potency towards rat N-type calcium channels ([80]) along with significant lower folding yields for the other two disulfide bonds ([81]). Lastly, disulfide bond isomer configuration is essential for bioactivity as well. For example, in α-conotoxins with two disulfide bonds in most cases favor the globular disulfide isomer for optimal potency. However, a rare issue has been found in α-conotoxin AuIB where the ribbon disulfide isomer resulted in 10 times greater potency towards the nAChR when compared to the native globular disulfide isomer ([82]).

Characterization of *C*-terminal amidation and disulfide bonding has been well established in proteomics. Identification of a *C*-terminal amide can be detected through a combination of oxazolone derivatization and tandem MS, with a 14 Dalton (Da) increase via the *C*-terminal PTM fragment ([83],[62]). Introducing a *C*-terminal amide also decreases the peptide mass 58 Da relative to its precursor (differ only by the *C*-terminal glycine) ([84]). Disulfide bond characterization can be confirmed via MS (-2 Da per disulfide bond) and analyzed via reversed-phase high-performance liquid chromatography (RP-HPLC) (shift in retention time shown on a chromatogram). Disulfide isomer arrangement is confirmed via NMR spectroscopy, RP-HPLC, and oxidation.

1.3.4 Proline Hydroxylation

The hydroxylation of proline (Hyp) is a PTM found in a wide range of plants and animals; found in collagen to stabilize the collagen triple helix and used in plants as a defensive system against herbivore attack ([85],[86]). There are greater than 85 *cis*- and *trans*-hydroxylated prolines found in naturally occurring conotoxins ([87]). However, the effect on the structure and bioactivity of this common PTM is not entirely understood.

A single mutation of proline to hydroxyproline in conotoxins gives mixed results. Lopez-Vera *et al.* tested this substitution synthetically in 4 different conotoxins; μ-GIIIA, ω-MVIIC, α-ImI, and α-GI. The results from the paper concluded; Hyp μ-GIIIA improved the ability to block sodium channels, Hyp ω-MVIIC had no effect on activity but increased folding yields, α-ImI and α-GI improved folding yields but significantly decreased activity to their corresponding receptors ([88]). The proline to hydroxyproline substitution in the α-conotoxins is most commonly found in the first disulfide loop. In α-conotoxins, the first disulfide loop, or *m* loop, is highly conserved and crucial for binding to the receptor ([89]) and could be considered the reason for such a steep decrease in activity.

Isobaric PTM αα's present high challenges in identification with low-resolution mass spectrometers (e.g. ion trap) ([90]). Hydroxyproline is isobaric with leucine and isoleucine at 131 Da. Methylated valine also has a molecular mass of 131 Da but has yet to be discovered in conotoxins. A similar issue has been seen in the PTMs sulfonation and phosphorylation, where both PTM's have a molecular weight of 80 Da ([91]). On another note, substituting proline to hydroxyproline has a mass increase of 16 Da. A mass increase of 16 Da may also be seen in the oxidation of methionine residue to sulfoxide ([92]). With similar monoisotopic mass distributions, Soltwisch *et al.* could discriminate isobaric leucine and isoleucine via high-energy matrix-assisted laser desorption ionization time-of-flight mass spectrometry (MALDI-TOF-MS) with collision cooling. This process generates side-chain degradation within αα, thus providing characteristic low abundant *w*- or *d*- ions ([93]). If there is no access to a MALDI-TOF-MS system, Langrock *et al.* could discriminate between the leucine, isoleucine, and hydroxyproline through αα analysis and a N_2-(5-fluoro-2,4-dinitrophenyl)-L-valine amide on collagen ([94]). This method was later confirmed via electrospray ionization (ESI) MS.

1.3.5 *N*-Terminal Truncation

N-terminal truncation, or truncation of conotoxins in general, has the advantage of structural simplicity with a less expensive and faster synthesis ([95]). Truncated peptides also present a more drug-like appearance with an economic advantage towards producing novel therapeutics ([96]). *N*-terminal truncation is the deletion of one or more αα before the first cysteine on the *N*-terminal. *N*-terminal deletion is observed throughout conotoxin families, with its recruitment adding another layer of diversity for receptor hindrance and prey paralysis. This modification also illustrates PTM is not restricted to only αα side chains ([97]). Synthetic modifications of *C*-terminal and inter-cysteine loop truncation are also seen in research but will not be focused on in this thesis. Results of this modification to functionality are varied and generally misunderstood.

There are multiple instances of *N*-terminal truncation within α-conotoxins (see Table 4). α-CnIB is milked from *Conus consors* and is the truncated form of α-CnIA (2 αα deletions from the *N*-terminal). The half-maximal inhibitory concentration (IC_{50}) confirmed bioactivity in α-CnIA towards the muscle nAChR, but no bioactivity assay was done on the truncated version ([98]). α-MIC is milked from *Conus magus* and is the truncated version of α-MI (2 αα deletion from the *N*-terminal). Kapono *et al*. determines the characterization of α-MIC and α-MI, as well as the development of *des*[Gly]^1 α-MI (1 αα deletion from the *N*-terminal of α-MI). All resulted in nanomolar affinity towards the muscle nAChR, but *des*[Gly]^1 α-MI and α-MI had about a 3-fold increase in affinity compared to α-MIC ([97]). Kapono *et al.* concluded the deletion of the positively charged arginine in α-MIC might contribute to the binding affinity towards the muscle nAChR. This abbreviates the importance of truncation as a tool to determine critical residues within a sequence. Synthetic *N*-terminal truncation is seen throughout many more papers, but the pharmacological importance remains to be established.

Table 4: α3/5 conotoxins with *N*-terminal truncation.

α-Ctx	Sequence
des-Ile-SI	**CC**NPA**C**GPKYS**C***
CnIB	**CC**HPA**C**GKYYS**C***
CnIC	**CC**HPA**C**GKHFS**C***
CnID	**CC**HPA**C**GKHFN**C***
[Hyp4] CnID	**CC**HOA**C**GKHFN**C***
CnIG	**CC**HPA**C**GKYFK**C***
des[Gly]^{1}MI	R**CC**HPA**C**GKNYS**C***
MIC	**CC**HPA**C**GKNYS**C***

**, C-terminal amidation; Ctx, Conotoxin; O/Hyp, 4-trans-hydroxyproline. Other than des[Gly]^{1} α-MI, all α-conotoxins listed were found natively within the piscivorous species. Cysteines are highlighted in bold.*

1.3.6 Bromination of Tryptophan

The halogen bromine (Br^-) is naturally abundant in marine environments. Concentrations of seawater bromide fall in the range of 60-80 mg kg^{-1} ([99]) and contribute to the high amount of bromine found in marine organisms. There are considered thousands of brominated compounds of biological origin, many of which are used as bioactive secondary metabolites in sessile organisms for predator defense (e.g. sponges, seaweeds, corals, hemichordates) ([100],[101]). The first brominated compound discovered in cone snails was analyzed by Olivera and his team ([102],[103]). The residue was considered a PTM of tryptophan, L-6-bromotryptophan to be exact, and is now found throughout many conotoxins.

Olivera and his team discovered three different conotoxins in 1997 that embedded an L-6-bromotryptophan; the bromocontryphan and bromosleeper conotoxin from *Conus radiatus* and the bromoheptapeptide from *Conus imperialis*. The bromoheptapeptide did not elicit any behavioral symptoms when injected into mice. However, the bromosleeper conotoxin induced a lethargic state in mice of all ages and the bromocontryphan conotoxin induced "stiff tail" syndrome in mice ([102],[103]). Selectivity has been examined in the bromosleeper peptide; Trp^1 is brominated while Trp^{25} is not ([102]). Although, comparison studies between native contryphan to

bromocontryphan resulted in no change of activity via the bromine addition. This has left investigators pondering the overall purpose of the evolutionary introduction of bromination in conotoxins.

There have been many different methods to identify the presence of bromotryptophan in novel conotoxin sequences. The bromoheptapeptide sequence was discovered after a non-identifiable 5th residue was observed during classical Edman degradation. cDNA encoding resulted in a parent tryptophan residue at this position ([102]), which in turn began the search for this novel PTM. In the same year with the bromosleeper peptide, two mono-isotopic forms of the parent mass existed and differed by 2 Da under standard MS conditions ([103]). Later analysis confirms this behavior due to 2 natural isotopic forms of Br^- existing in seawater. Comparative analysis between native versus synthetic of the bromoheptapeptide and bromosleeper peptides observed; same MS parent masses (similar mono-isotopic mass distribution of the bromosleeper peptide) and co-elution via RP-HPLC retention times. Other identifications of bromination use a combination of sequence analysis, cDNA cloning, MS techniques, and NMR characterization ([104],[105]).

1.3.7 Non-Native αα Integration

Generating new sequences to maximize existing conotoxin families as a parent template allows much potential in peptide drug development ([65]). A single mutation within a conotoxin sequence can have dramatic effects on receptor specificity, peptide folding and overall bioactivity. As seen with many peptide drugs in the market today, chemical manipulation of peptide structure can provide that extra step from native peptide to drug candidate ([106]). The introduction of non-native αα into conotoxin sequences is one avenue that can result advantageous.

1.4 *Conus obscurus*

Conus obscurus is a piscivorous cone snail that has a species distribution from the Indo-Pacific region (Hawai‘i and French Polynesia), Indian Ocean, and off the coasts of Australia and the Philippines. *C. obscurus* has not been thoroughly studied due to; (i) the rarity of the snail that limits research and (ii) the small size of the snail (see Figure 5) that correlates with a low yield in venom collection from the duct and milked venoms. In addition, intra- and inter-species diversity among other *Conus* species and specimens guarantee an abundance of peptides to be analyzed ([107]).

Figure 5: *Photo of* Conus obscurus *shell found off of the Hawaiian Islands, USA.*

Scale bar 1 cm.

Through a literature search, only ~10 peptides have been documented from the venom of *C. obscurus*. Of those peptides, half originate from cDNA clones (only the primary sequence is known). The two conotoxins that have been pharmacologically characterized from *C. obscurus*, α-OIVA and α-OIVB, belongs to the αA-conotoxin superfamily and demonstrate selectivity towards the fetal neuromuscular nAChR (αβγδ). Although, both show a much lower affinity to the adult neuromuscular nAChR (αβϵδ) and virtually no inhibitory effects towards the neuronal nAChRs ([108],[109]).

1.5 Aims and Objectives

This thesis was undertaken to build upon the discovery of 2 αA-conotoxins found from the milked venom (MV) of *Conus obscurus*; one novel (α-ObI) and one previously found in the venom of *Conus striatus* (α-SI). Once the α-ObI sequence is confirmed, α-ObI and several analogs of the peptide go through rounds of synthesis, oxidation and purification. Once purified, α-ObI and analogs will go through 2 animal bioassays to be pharmacologically characterized. The underlying hypothesis of this thesis is α-ObI can be mutated to increase overall potency towards the muscle-type nAChR, as well as incorporate PTMs to ultimately investigate the boundaries of peptide bioengineering in the generation of novel α-conotoxins.

Chapter 2 Methods

2.1 Venom Extraction and Analysis

Conus obscurus was housed in an aquatic system developed by Milisen et al. ([110]) and milked via methods implemented by Hopkins et al. ([111]). Singular venom extractions was collected, pooled, and analyzed via RP-HPLC using Waters Alliance 2695 coupled with a 996 Waters Photodiode Array (PDA) detector and an analytical Vydac column (5 µm particle, 300Å pore, 2.1 x 250 mm). The pooled MV was desalted via preparative RP-HPLC with a 2 mL min^{-1} isocratic flow of Solvent A (0.1% trifluoroacetic acid (TFA) aq.) water followed by 80/20 v/v acetonitrile (MeCN) and 0.08% TFA aq. Material elution was monitored at 214 nm with preparative setup described by Bergeron *et al*. ([110]). The sample was again freeze-dried and reconstituted in TFA water for storage at -20 °C.

Figure 6: Project map of the extraction to the sequencing of α-SI and α-ObI.

LC-MS/MS and fractionation/purification were executed concurrently.

2.2 Mass Spectrometry (MS) Techniques and Sequencing

The pooled sample of parent masses was observed via ESI-MS to determine known and unknown peptides observed from the RP-HPLC chromatograms. Conoserver was consulted for known *C. obscurus* peptides and their parent masses. From these results, the peaks resembling α-SI and α-ObI were chosen for purification, both of which were analyzed by MALDI-TOF by multiple interpreters.

In addition, ~5% of the master sample underwent LC-MS-MS methods through direct injection of rough fractions into an AB/MDS Sciex API 3000 triple quadrupole mass spectrometer. The desalted peptide was analyzed on a Bruker nanoLC-AmaZon speed electron transfer dissociation (EDT) ion trap mass spectrometer system (Bruker Daltonics Inc., Fremont, Ca.) and separated via a C_{18} analytical column. Fragmentation data were acquired in EDT and collision-induced dissociation (CID) mode.

A MaXis Impact Q-TOF mass spectrometer interfaced with a Michrom Advance Nano LC was used to collect LC-MS-MS data on the pooled peptide mix. A Bruker Ultraflex III MALDI-TOF instrument was used in conjunction with Compass 1.2 SR1 software to collect data on purified peptides.

In addition, FlexAnalysis v3.0 was used to sequence peptides manually. Data was also sent to the University of Alberta Chemistry Department for blind interpretation using FlexAnalysis. The department investigator was not informed of the species but was informed that the genus was *Conus*.

2.3 Peptide Synthesis

Once the α-ObI sequence was confirmed, the novel sequence and five analogs underwent 9-Fluorenylmethoxycarbonyl solid-phase peptide synthesis (fmoc-SPPS) chemistry. Synthesis of contrived linear peptides accompanied by standard αα side protection, except for the four cysteines. Fmoc αα was measured with 4-fold excess (2 mM) compared to a CLEAR-Amide resin (.5 mM) at 0.47 meq g-1 with a 15 min. coupling time. Although, 15% excess (2.3 mM) of

Fmoc-5-Bromo-L-tryptophan with a 60-min. coupling time was used to allow for optimal non-native αα integration.

General synthesis protocol was adapted by Kapono *et al.* ([97]). The CLEAR-Amide resin was swelled and shaken in 4 mL dimethylformamide (DMF) overnight. The resin was washed effectively with DMF (3 x 20 mL), deprotected with 50% v/v piperidine in DMF (2 x 5 mL), and again washed effectively with DMF (3 x 20 mL). Fmoc αα were activated in-situ via (mL) HBTU/DMF until completely dissolved, then mixed with 347 mL (2 mM) N,N-Diisopropylethylamine (DIEA). The activated αα was then added to the resin and coupled for 15 min. After coupling, a ninhydrin test was performed ([112]). A NanoDrop™ ND-1000 spectrophotometer measured the percent coupling of the αα to the resin. Once percent coupling was ≥ 99.5%, the resin and peptides were washed and deprotected as described above. The next αα in the peptide sequence was then activated as described above. Once the full peptide sequence was constructed from the *C*-terminus to the *N*-terminus, the peptide was then washed with DMF (3 x 20 mL), washed with dichloromethane (DCM) (5 x 20 mL), and dried under N_2 gas.

The resulting peptide was then added to Reagent K (82.5% TFA, 5% phenol, 5% DI water, 5% thioanisole, 2.5% 1,2-ethanedithiol) in a ratio of 30:1 mL g^{-1} for 2 hrs. The resin was filtered, and the peptide precipitate was separated (10 mL) into falcon tubes with the addition of chilled tert-butyl methyl ether. Peptide precipitate was pelleted by centrifugation (3000 g, 4 °C, 10 min) and washed 2 more times with fresh chilled tert-butyl methyl ether. After all the ether was discarded, the peptide pellet was suspended in 25% v/v acetic acid freeze-dried overnight. The resulting peptide will take on a powdered form and be then put under oxidation.

2.4 Peptide Oxidation

Oxidation differs between a-ObI and the five analogs. a-ObI contained four S-trityl (trt) protected cysteines from undergoing random disulfide folding, while analogs contained two S-trt and two acetamidomethyl (acm) protected cysteines in a certain order to take on the preferred globular isomer structure found natively in a-ObI.

a-ObI is oxidized before analogs to confirm the preferred isomer structure. Most a3/5 conotoxins take on the globular isomer structure, but in rare cases you may find a-conotoxins in the beaded or ribbon isomer structure. a-ObI was put under nine different oxidation conditions with different components, pH, temperature, and durations. Through RP-HPLC analysis, the condition with the highest yield of the preferred globular isomer was analyzed. The linear form of a-ObI was spun under the preferred condition (0.1 M ammonium bicarbonate (NH_4HCO_3); pH 8; 25 °C, five days) at a 1:10 ratio m/v. After five days, 100% acetic acid was added dropwise until the pH of the solution was < 4. The oxidation process facilitated random folding and the formation of intrachain disulfide bonds, producing the three-dimensional structure of the peptide. Lastly, the oxidized material was desalted via semi-preparative RP-HPLC and freeze-dried overnight. Purification is followed on analytical RP-HPLC to retrieve a pure, toxic a-ObI conotoxin.

The five analogs presented will undergo selective disulfide folding. The first oxidation is the same condition used to fold a-ObI. This will deprotect the 2 S-trt cysteines and form the first disulfide bond. The partially oxidized material will then undergo second and final oxidation (thiol deprotection). This final oxidation will remove the two acm protected cysteines and form the second disulfide bond. Iodine crystals (21 mg) were crushed into a fine powder and dissolved in 840 uL of 100% acetic acid. In a separate vial, 1-5 mg of the peptide was dissolved in 2 mL of 50% v/v acetic acid. 600 uL of saturated iodine solution was gradually added and vortexed. After 5 min., the reaction is terminated by the dropwise addition (4 uL) of 1M sodium thiosulfate ($Na_2S_2O_3$) until the solution is colorless. The mixture is quenched by 5-7 mL of 0.1% v/v TFA aq. The peptide was purified and desalted by preparative RP-HPLC, analyzed by analytical RP-HPLC, and confirmed monoisotopic mass by ESI-MS before and after each oxidation.

2.5 Chromatographic Separation and Analysis

Native and synthetic conotoxins were individually separated as follows: (i) Capillary Scale (Phenomenex; C-18, 5 μm, 300 Å, 1.0 × 250 mm, flow 100 μL $min.^{-1}$) - used for comparative RP-HPLC/UV (ultraviolet) profiling, to control the quality of peptide purity, to quantify the peptides and to perform peptide co-elution experiments. (ii) Analytical Scale (Vydac; C18, 5 μm, 300 Å, 4.2 × 250 mm, flow 1 mL $min.^{-1}$) - used for the isolation and

purification of native peptides for MS analysis. (iii) Preparative Scale (Vydac; C^{18}, 10 µm, 300 Å, 22 × 250 mm, flow 5 mL $min.^{-1}$) -used for the preparative separation of crude synthetic peptides for co-elution experiments, structure determination, and pharmacological assays. Systems (i) and (ii) used a Waters 2695 Alliance RP-HPLC System interfaced with a 996 Waters PDA Detector for automated sample analysis and detection. Data was acquired and analyzed using Waters Millennium^{32} (v3.2) software. Samples were eluted using a linear 1% $min.^{-1}$ gradient of organic Solvent B (90/10% v/v MeCN/0.08% v/v aq. TFA) against aqueous Solvent A (0.1% v/v TFA aq.) for 65 min., excluding a terminating high organic wash (80% Solvent B for 5 min.), and pre-equilibration step (5% Solvent B) for 10 min. prior to sample injection. The eluent was monitored from 200–300 nm and extracted at 214 nm. Preparative RP-HPLC/UV system (iii), used a 625 Waters HPLC pump and controller interfaced with a 996 Waters PDA Detector. Both gradient control and data acquisition were facilitated by the use of the Waters Millennium^{32} software. Filtered (Nylon 0.22 µm) synthetic peptides and crude venom peptide extracts were manually loaded and eluted from the preparative scale column using the same 1% gradient at 5 mL $min.^{-1}$ and monitored at 214 and 280 nm. Fractions were collected manually and stored at −20 °C or freeze-dried until required.

2.6 Amino Acid Analysis

Once a pure, oxidized, and freeze-dried sample of each peptide was obtained, peptides were then sent to the UC Davis Molecular Structure Facility to undergo αα analysis. Peptides were quenched 2x 200 uL formic acid/ACN and transferred (entire sample) to liquid phase hydrolysis (200 µL 6N HCl/1% phenol at 110 °C for 24 hrs.). Once hydrolyzed, the sample was then dissolved in NorLeu dilution buffer and vortexed/spun down. 50 µL of the sample was then loaded into an L-8800 Hitachi αα analyzer. Ion-exchange chromatography was used to separate αα, followed by a "post-column" ninhydrin reaction detection system to quantify individual αα. Peptides were presented in [nM $µL^{-1}$].

2.7 Fish Bioassay (LD_{50})

Injection of α-ObI and analogs into fish (*Poecilia reticulata*) were made to find peptide median lethal dose (LD_{50}) concentrations. Peptide concentrations ranged from 20, 10, 5, 2.5 and 1 nmol g^{-1} in 1x phosphate buffered saline (PBS). 5 µL injections were administered

intramuscularly into the fish via a Hamilton microliter syringe. Methods were adopted by Meier *et al.* ([113]) to reduce experimental animal numbers.

Ten 0.11- 0.20 g fish were injected for each peptide assay. The range consists of three different increasing dosage (D) concentrations with three fish per dose (one control). Survival times (T) were recorded in seconds from the time of injection to observed death. A scatter plot was composed with D/T [(μg/g)/ seconds] as the independent variable versus D (μg/g) as the dependent variable. A regression line (y=mx+b) is found and m (slope) and b (LD_{50}) of the line are obtained through calculation ([113]).

2.8 Functional characterization (EC_{50})

2.8.1 Expression of Voltage-Gated Ion Channels in *Xenopus Laevis* Oocytes

For the expression of human AChR (α1, α3, α4, α7, α9, α10, β2, β4, γ; δ; ε) in *Xenopus laevis* oocytes, the linearized plasmids were transcribed while using the T7 or SP6 mMESSAGE-mMACHINE transcription kit (Ambion®, Carlsbad, CA, USA). The harvesting of stage V–VI oocytes from anesthetized female *Xenopus laevis* frog was previously described ([114]). Oocytes were injected with 50 nL of cRNA at a concentration of 1 ng nL^{-1} using a micro-injector (Drummond Scientific®, Broomall, PA, USA). The oocytes were incubated in a solution containing (in mM): NaCl, 96; KCl, 2; $CaCl_2$, 1.8; $MgCl_2$, 2; and HEPES 5 (pH 7.4), supplemented with 50 mg L^{-1} gentamicin sulfate.

2.8.2 Electrophysiological Recordings

Two-electrode voltage-clamp recordings were performed at room temperature (18–22 °C) while using a Geneclamp 500 amplifier (Molecular Devices®, Downingtown, PA, USA) controlled by a pClamp data acquisition system (Axon Instruments®, Union City, CA, USA). Whole-cell currents from oocytes were recorded 1–4 days after injection. Bath solution composition was (in mM): NaCl, 96; KCl, 2; $CaCl_2$, 1.8; $MgCl_2$, 2; and HEPES 5 (pH 7.4). Voltage and current electrodes were filled with 3 M KCl. Resistances of both electrodes were kept between 0.7 and 1.5 MΩ. During recordings, the oocytes were voltage-clamped at a holding potential of −70 mV and continuously superfused with ND96 buffer via gravity-fed tubes at 0.1–

0.2 mL $min.^{-1}$, with 5 min. incubation times for the bath-applied peptides. Acetylcholine (ACh) was applied via gravity-fed tubes until peak current amplitude was obtained (1–3 s), with 1–2 min. washout periods between applications. The nAChRs were gated by a variable time duration pulse of ACh (200 μM for αβγδ, α4β2, α4β4, αβδε; 100 μM for α7; and, 500 μM for α9α10) for the different nAChR subtypes at 2 mL min^{-1}. Data was sampled at 500 Hz and filtered at 200 Hz. Peak current amplitude was measured prior to and following the incubation of the peptide.

To assess the concentration-response relationships, data points were fitted with the Hill equation: $y = 100/[1 + (EC_{50}/[toxin])h]$, where y is the amplitude of the toxin-induced effect, EC_{50} is the toxin concentration at half-maximal efficacy, [toxin] is the toxin concentration, and h is the Hill coefficient. A comparison of two sample means was made using a paired Student's t-test ($p < 0.05$). The data are presented as mean ± standard error (SEM) of at least six independent experiments ($n \geq 6$). All the data were tested for normality using a D'Agostino-Pearson omnibus test. All the data were tested for variance while using the Bonferroni test or Dunn's test. Data following a Gaussian distribution were analyzed for significance while using a one-way analysis of variance (ANOVA). Non-parametric data were analyzed for significance using the Kruskal–Wallis test. Differences were considered to be significant if the probability that their difference stemmed from chance was < 5% ($p < 0.05$). All data was analyzed while using pClamp Clampfit 10.0 (Molecular Devices®, Downingtown, PA, USA) and Origin 7.5 software (Originlab®, Northampton, MA, USA).

Chapter 3 Results

3.1 Discovery of *Conus obscurus* 1 from Milked Venom

MV from *Conus obscurus* was obtained and analyzed for novel bioactive peptide sequences in the Bingham Laboratory from the University of Hawai‘i, Mānoa. Over 250 MVs were observed via RP-HPLC, but two main peaks are discerned for this thesis (refer to Figure 7). The first peak is at t_R=31 min 1357.62 *m/z*, which is a documented alpha conotoxin previously discovered from the venom of *C. striatus*. The other peak is at t_R=33 min 1400.56 *m/z*, which is a novel peptide sequence that will be regarded as the main sequence for synthetic peptide engineering. Peptide sequence data was discovered using ESI-MS and MALDI-TOF-MS. Peaks6 program was used to sequence peptides de novo from the ESI-MS ([115]). MALDI-TOF-MS data was manually interpreted and then sent to the University of Alberta Chemistry Department to interpret blinded.

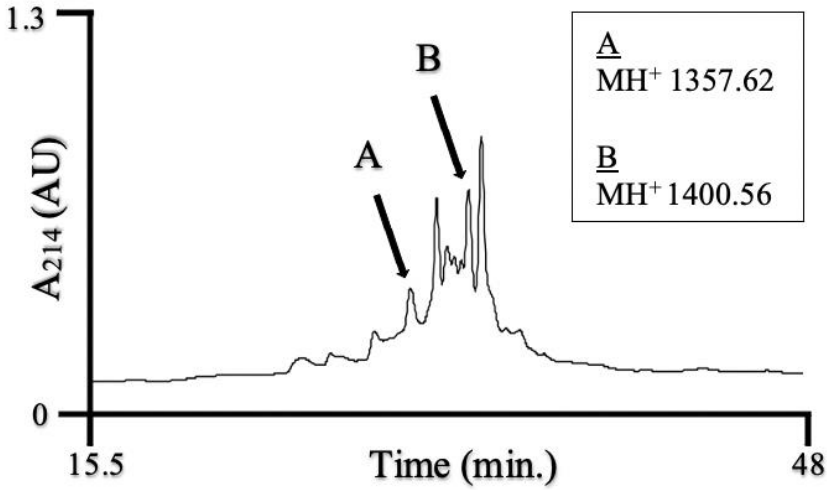

Figure 7: TCEP reduced, pooled milked venom profile via RP-HPLC at 214 nm.

The two discovered peptides (peak A and B) with the corresponding MH+ (monoisotopic mass). The chromatogram was completed by Sugai et al. ([115]).

3.1.1 1357 *m/z* Sequencing

Alpha conotoxin SI has been previously discovered in *C. striatus* and described by Zaffaralla et al. ([116]). The sequenced determined from MALDI-TOF in-house (University of Hawai‘i) sequencing was distinct from Peaks6 confidence levels of 1357.62 *m/z* at the C-terminal. Sequence data was also sent to the University of Alberta without interpretation (refer to Figure 8 and Table 5); the sequence generated was duplicated with manual in-house sequencing data. Both interpreters agreed 1357.62 *m/z* is a direct match with α-SI when considering the first αα is isoleucine instead of leucine, as these isobaric αα are difficult to differentiate from mass spectrometry data. The conotoxin α-SI is considered an α3/5 alpha conotoxin based on its cysteine framework XCCX3CX5C. Table 5 and Figure 8 were obtained from Sugai's thesis ([115])

Table 5: Peptide sequence results from 1357.62 *m/z*.

Sequence	Source
(I/L)CCNPACGHLC*	Peaks6
(I/L)CCNPACGPKYSC*	University of Alberta
(I/L)CCNPACGPKYSC*	University of Hawai‘i

*, *C-terminal amidation*

University of Hawai‘i

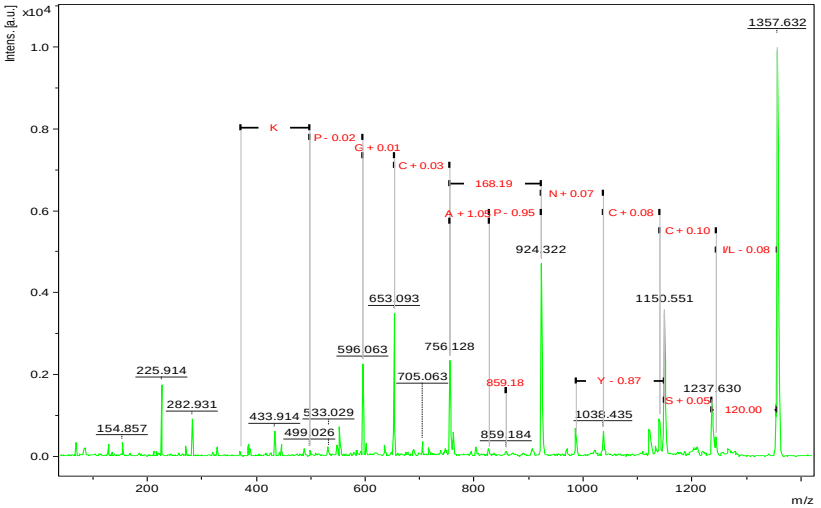

University of Alberta

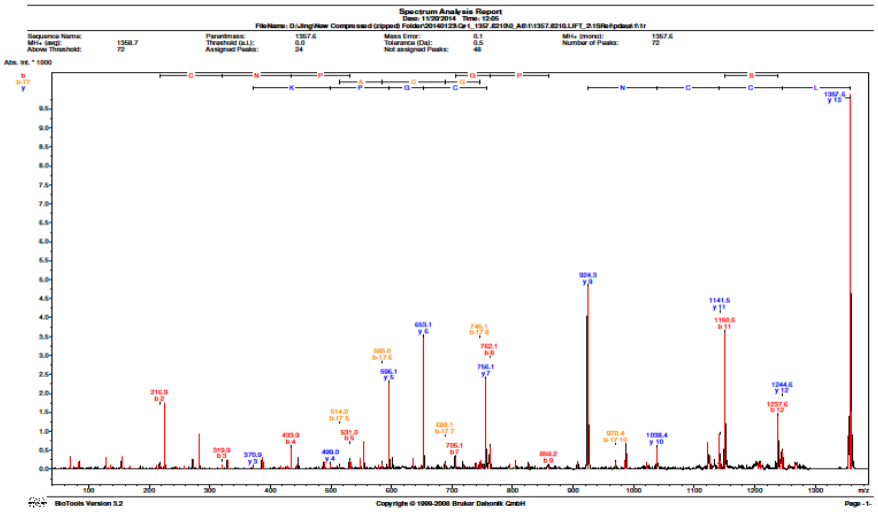

Figure 8: MALDI-TOF analysis of 1357.62 *m/z* peptide between interpreters.

Comparison between the University of Hawai‘i in-house sequencing versus the University of Alberta blind interpretation sequencing of 1357.62 m/z. Both sequences interpreted the C-terminal amidated (I/L)CCNPACGPKYSC.

3.1.2 1400 *m/z* Sequencing

A novel peptide was discovered at peak 1400.56 *m/z* from Sugai's RP-HPLC data (refer to Figure 7). For this thesis, the 1400.56 *m/z* peptide will be referred to as *Conus obscurus* 1, or α-ObI. Between the 3 sequencing techniques in Table 6, there was an ~85% confirmation on the sequence generated from the University of Hawai'i. As you can see from Figure 9, the in-house MALDI-TOF data has an unexplained peak at 835.139 *m/z*, resulting in a 12 αα peptide. Since the University of Alberta had corroborating peaks and has the 835.1 *m/z* characterized as an αα, we can confirm the University of Alberta's sequence was presumed correct.

Table 6: Peptide sequence results from 1400.56 *m/z*.

Sequence	Source
HCCYPACGPNHCP*	Peaks6
YCCHPACGPNFSC*	University of Alberta
YCCHPACDHYSC*	University of Hawai‘i

*, *C-terminal amidation*

University of Hawai‘i

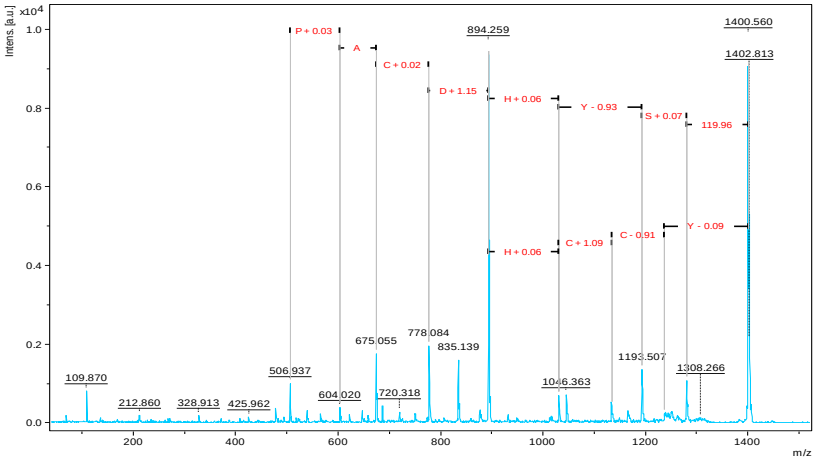

University of Alberta

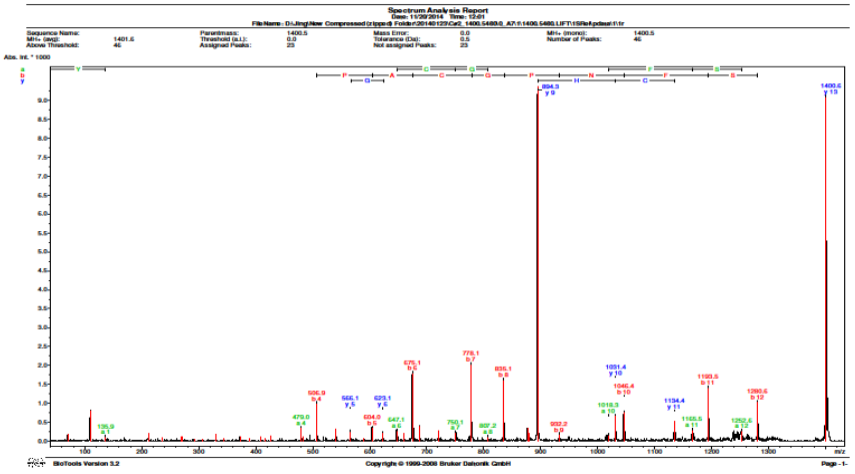

Figure 9: MALDI-TOF analysis of 1400.56 *m/z* peptide between interpreters.

Comparison between the University of Hawai‘i in-house sequencing versus the University of Alberta blind interpretation sequencing of 1400.56 m/z. Interpretation of sequenced differed due to an unexplained peak in the University of Hawai‘i sequence. The unexplained peak was resulted by University of Alberta, confirming their sequence was correct. Their sequence interpreted a C-terminal amidated YCCHPACGPNFSC.*

A BLAST search of University of Alberta's presumed correct sequence confirms the similarity between this novel sequence and many other alpha conotoxins (Table 7). α-ObI is a confirmed α3/5 alpha conotoxin with a single mutation difference between a peptide found in *C. striatus* and *C. stercusmuscarum* (F in ObI exchanged with a Y). α-ObI also has a two-mutation difference compared to α-GII, α-MI, and the precursor α-S1.10b.

Table 7: BLAST results from the alignment of α-ObI.

BLAST ObI alignments	BLAST comparison	Score	E-Value	Per. ID	Source
Superfamily Ctx [*Conus Striatus*]	Query 1 YCCHPACGPNFSC 13 YCCHPACGPN+SC Sbjct 47 YCCHPACGPNYSC 59	46.9	6e-05	92.31%	Genetic
Alpha-Ctx-like Sm1.1 [*Conus stercusmuscarum*]	Query 2 CCHPACGPNFSC 13 CCHPACGPN+SC Sbjct 48 CCHPACGPNYSC 59	42.6	0.002	91.67%	Milked Venom
Alpha-Ctx SIA [*Conus striatus*]	Query 1 YCCHPACGPNFSC 13 YCCHPACG NF C Sbjct 1 YCCHPACGKNFDC 13	39.7	0.003	84.62%	Milked Venom
Superfamily Ctx, partial [*Conus striatus]*	Query 1 YCCHPACGPNFSC 13 YCCHPACG NF C Sbjct 25 YCCHPACGKNFDC 37	39.7	0.017	84.62%	Genetic
Superfamily Ctx S1.10b precursor [*Conus striatus*]	Query 1 YCCHPACGPNFSC 13 YCCHPACG NF C Sbjct 50 YCCHPACGKNFDC 62	39.7	0.022	84.62%	Genetic
Alpha-Ctx MI [*Conus magus]*	Query 2 CCHPACGPNFSC 13 CCHPACG N+SC Sbjct 3 CCHPACGKNYSC 14	36.7	0.047	83.33%	Milked Venom
Alpha-Ctx GII [*Conus geopraphus*]	Query 2 CCHPACGPNFSC 13 CCHPACG FSC Sbjct 2 CCHPACGKHFSC 13	36.3	0.063	83.33%	Milked Venom
Alpha-Ctx SI [*Conus striatus*]	Query 2 CCHPACGPNFSC 13 CC PACGP +SC Sbjct 2 CCNPACGPKYSC 13	35	0.22	75.00%	Milked Venom

Ctx; Conotoxin. The top two hits had a single mutation difference in position 11. The top four duct venom alignments in order are as follows; α-Sm1.1, α-SIA, α-MI, α-GII, α-SI.

3.2 Development of α-ObI Analogs

3.2.1 α-ObI and the α3/5 Conotoxin Subfamily

Alpha conotoxins with the cysteine framework of α3/5 affect the neuromuscular (muscle-type) nAChR found at the neuromuscular junction. Since α-ObI is considered an α3/5, it would be safe to assume that this peptide affects the muscle nAChR, specifically the αβδγ/ε subunit. Also, the α3/5 subfamily has a high specificity for the αβδ interface of the mammalian muscle nAChR ([117]). α3/5 conotoxin α-GI and α-MI has a 10,000-fold greater affinity for the αβδ site (compared to the αβγ site) in BC3H-1 mouse receptors ([118], [119]). In that case, it would also be safe to assume there would be a higher IC_{50} for α-ObI on the mammalian muscle αβδ subunit, rather than the αβγ site.

The α3/5 subfamily of *Conus* has a relatively narrow sequence spectrum as illustrated in Figure 10. From a bioengineering perspective, a bioinformatics approach is needed to understand which αα positions crucially affect the binding of the peptide to the muscle nAChR. Individually examining each position in every documented α3/5 sequence to see how this position affects toxicity, dissociation rate, binding affinity, etc. can give the reader a better understanding of this paralytic subfamily of conotoxins.

Figure 10: The α3/5 conotoxin consensus sequence.

The consensus sequence was developed by Jacobsen et al. ([117]). Black residues are generally conserved, while red residues are variable. The residue X (any amino acid) in position 1 does not have 2 favorable αα like the ones shown in positions 4 and 9-11.

Positions 1, 4, and 9-11 are considered to have the highest hypervariability in the α3/5 conotoxin sequences. The process of determination of α-ObI analogs is featured in Figure 11, which illustrates a mind map to determine the best possible analogs to increase overall potency and selectivity. The five conotoxins branching off of the α-ObI sequence in Figure 11 are the most engineered α3/5 conotoxins found today. However, numerous other α3/5 conotoxins (25+) were also observed in the determination of α-ObI analogs.

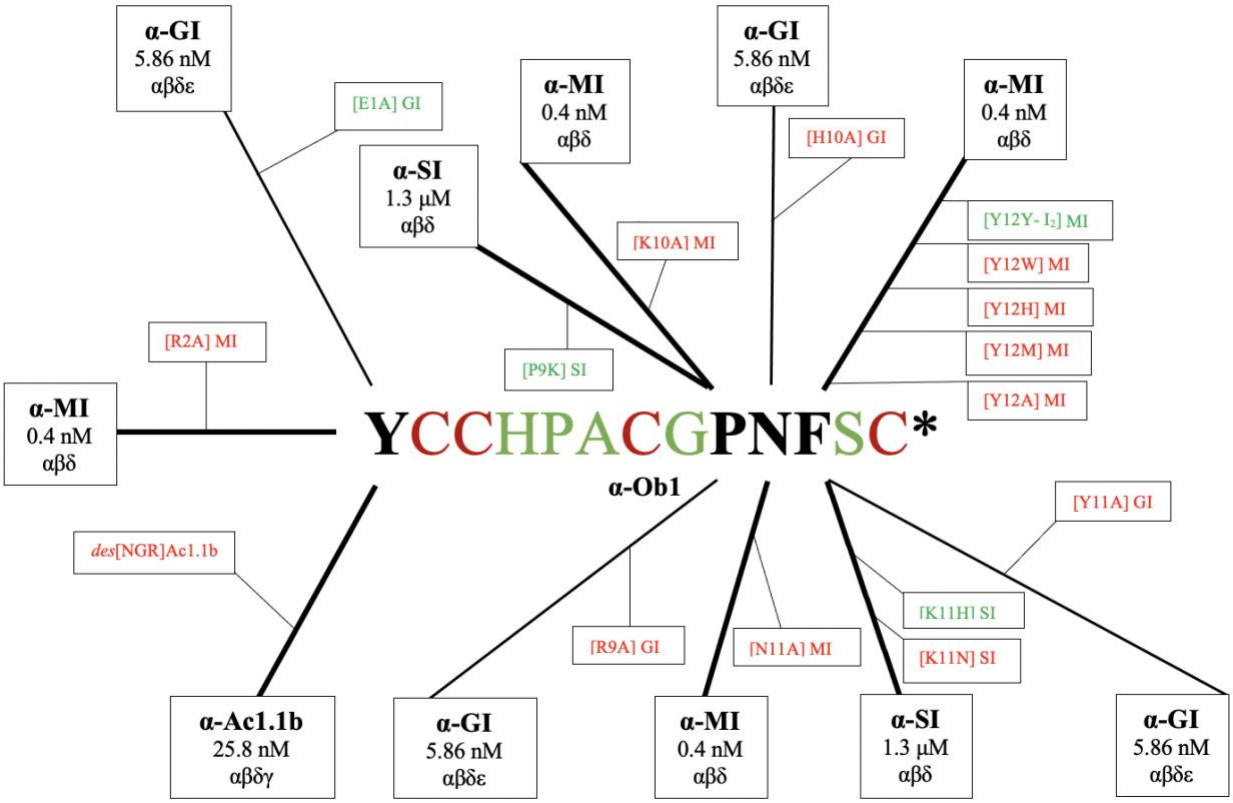

Figure 11: A site-specific mutational map of α3/5's compared to the α-ObI sequence.

Within the α-ObI peptide sequence, the bold αα is variable while the green αα is generally conserved (cysteines highlighted in red). Branch width is dependent on homology, with the wider branches being more homologous towards the α-ObI sequence. The long branch signifies the α-conotoxin, while the short branch coming off of the long branch is the analog. A red analog means the mutated conotoxin IC_{50} increased (less toxic) and a green analog means the mutated conotoxin IC_{50} decreased (more toxic). The number within the α-conotoxin boxes indicates the IC_{50} readings towards the M. musculus muscle nAChR subtype.

Positions 9, 10 and 11 in the second disulfide loop are highly variable throughout the α3/5 subfamily and have shown to be significant in terms of species specificity and the blocking of the muscle nAChR. These regions would be expected to have the largest backbone conformational changes. However, as shown in the root-mean-square deviation (RMSD) value, positions 9 and 10 have the highest degree of similarity in their solution structure than when compared to any other regions on the sequence ([120]). Altogether, there are 4 important residue components that are relevant to toxicity and affinity in the second disulfide loop; structure, hydrophobicity, polarity, and electrostatic charge. Minor adjustments to these four components may have an imperative influence on conotoxin potency/selectivity to the mammalian muscle nAChR.

Five analogs of the α-ObI parent template will be developed and are shown below in Table 8. Of the five analogs, there is a range of one to two mutations per analog and an overall introduction of 3 PTMs; proline hydroxylation, *N*-terminal truncation, and tryptophan bromination. Mutations found in each analog will have an *n* loop substitution, with one analog accompanied by an *N*-terminal deletion mutation. Each mutation has a purpose of increasing specificity towards the muscle nAChR, with the highest specificity is assumed in α-[P9K] [F11Br-W] ObI. Each analog will be represented in the following sections.

Table 8: The list of α-ObI analogs.

α-Ctx	Sequence
ObI	YCCHPACGPNFSC*
[P9O] ObI	YCCHPACGONFSC*
des[Y] [P9O] ObI	CCHPACGONFSC*
[P9K] ObI	YCCHPACGKNFSC*
[P9K] [F11W] ObI	YCCHPACGKNWSC*
[P9K] [F11Br-W] ObI	YCCHPACGKN(Br-W)SC*

**, C-terminal amidation; des, N-terminal truncation; Br-W, 5-Bromotryptophan; Ctx, Conotoxin; O, trans-4-hydroxyproine. A comparison between the novel α-ObI sequence and the five corresponding analogs was developed. The αα highlighted in red are the single and double mutations introduced to the α-ObI sequence.*

3.2.2 The Conserved Positions

The two disulfide loops, also represented as *m* and *n*, contain a 3 and 5 αα variety between the cysteines. It is generally known that the first disulfide loop *m* is crucial for binding, while the second disulfide loop *n* is responsible for selectivity due to pairwise interactions with the muscle nAChR subunits ([121], [122]). All muscle-specific α-conotoxins contain four hydrophobic αα that are highly essential for bioactivity; Pro-6, Ala-7, Gly-9 and Tyr-12 (positions relative to α-MI) ([123]). This section of the thesis will focus on the importance of Pro-5, Ala-6, and Gly-8 (the importance of position 11 will be described in the upcoming sections). Table 9 below shows the IC_{50} mutational change of these highly significant residues.

The *m* loop has three highly conserved residues; (H/N)PA. Position 4, the H/N residue, is assumed to have little effect on biological activity and will be further explained in the next section. However, Pro-5 is crucial to the 3_{10}-helix turn for forming α-conotoxins ([124]). Dutertre *et al.* demonstrate how the 3_{10}-helix turn may play an essential role in defining both the ligand conformation and receptor-binding activity in α-conotoxins ([125]). Data demonstrating alanine scan mutagenesis in position 5 for α-conotoxins MI/GI are shown below in Table 9. Jacobsen *et al.* and Ning *et al.* show an alanine mutation in position 5 results in a dramatic reduction in the

α3/5 conotoxins toxin potency at the muscle nAChR ([117], [124]). Ning *et al.* suggest the high reduction in potency in α-[P5A] GI is due to altering the β-turn secondary structures from Gly-8 to Tyr-11 ([124]).

Ala-6 is the second conserved αα in the *m* loop that is highly essential for α-conotoxin bioactivity for the muscle nAChR. Bren *et al.* show a significant reduction in affinity for the αβδ subunit with α-MI of nearly 10,000-fold decrease from Ala-7 substitution to Val-7 ([123]). Ala-7 in α-MI (Ala-6 in α-SI/GI) couples strongly to residues in both the αβδ and αβγ subunits, while Gly-9 and Tyr-12 prefer coupling to residues in the αβδ subunit ([123]).

Gly-8 in the second disulfide loop is highly conserved throughout all α3/5 conotoxins. Pro-5 in the *m* loop has a strong hydrophobic interaction with Gly-8 and the residues at the αβδ binding site in α-MI ([126]). This interaction appears to be one of the main stabilizers in α-conotoxin/nAChR binding. The small size of glycine in this position is crucial for the high affinity of these conotoxins ([122], [127]). As you can see from Table 9, Ning *et al.* show a 34-fold decrease in potency for α-[G8A] GI substitution for the adult muscle nAChR in mice ([124]). Further studies have shown decreases in potency via substitutions for Gly-8 in the fetal muscle nAChR ([128], [123]).

The recently discovered α3/5 conotoxin from *Conus milneedwardsi* named α-MiIIA has relatively low toxicity to both adult and *Homo sapiens* muscle nAChR ([114]). Instead of demonstrating the importance of Gly-8 via alanine scan mutagenesis in α-GI, Peigneur *et al.* had the ability to demonstrate the importance of Gly-8 by substituting the original residue methionine with the conserved glycine residue ([114]). As shown below in Table 9, the single mutation α-[M9G] MiIIA was able to increase the IC_{50} from micro to nanomolar range for the fetal muscle nAChR, but remained in micromolar range for the adult muscle nAChR ([114]). Toxicity was enhanced at both fetal and adult muscle nAChR from a double mutation α-[M9G, N10K] MiIIA and has the greatest toxicity at a 5 αα mutation α-[Δ1,M2R, M9G, N10K, H11K] MilIA ([114]).

Table 9: Muscle nAChR IC_{50} readings of the various α-conotoxins with conserved residue mutations.

α-Ctx	αδβ (nM)	αβγ (μM)	αβδε (nM)	αβδγ (nM)	Ref.
MI	0.4 ± 0.17	18 ± 5	-	-	[117]
[P6A] MI	19 ± 2	129 ± 32	-	-	[117]
GI	-	-	5.86 (5.01-6.86)	-	[124]
[P5A] GI	-	-	54.72 (46.85-63.91)	-	[124]
[G8A] GI	-	-	170.60(134.60-216.30)	-	[124]
[S12A] GI	-	-	5.39 (4.72-6.15)	-	[124]
MiIIA	-	-	11,180 ± 78,891	13,130 ± 1,125	[114]
[M9G] MiIIA	-	-	>50,000	577 ± 79	[114]
[N10K] MiIIA	-	-	>50,000	3,842 ± 148	[114]
[Δ1,M2R, M9G, N10K, H11K] MiIIA	-	-	25 ± 1	16 ± 1	[114]
[M9G, N10K] MiIIA	-	-	149 ± 39	178 ± 57	[114]

Δ1, Position 1 deletion; Ctx, Conotoxin. α-Conotoxin IC_{50} readings with mutations in the conserved positions of the α3/5 consensus sequence. The IC_{50} readings were tested on mouse muscle nAChR subunits. However, the native α-MiIIA and analog sequences were tested on Homo sapiens muscle nAChR,

3.2.3 Positions 4 & 10 in the α-ObI Sequence

Position 4 in the α-ObI sequence is histidine. All the native conotoxins in the α3/5 subfamily either contain a histidine or an asparagine in position 4. This position is the most conserved out of the red variable regions shown in the consensus sequence (see Figure 10), but it is the highest variable position in the first disulfide loop. As you can see from Table 10, there have been no significant changes in alanine scan mutagenesis in this position. Gray *et al.* states that the substitution between Asn-4 and His-4 is unlikely to be major determinant of the increased biological activity of α-MI to α-GI ([129]). For this thesis, histidine will remain the same throughout the development of all analogs of α-ObI.

The residue in position 10 of ObI is asparagine and alternates between histidine, tyrosine, and lysine in the other α3/5 subfamilies. Position 10 has had varied opinions as to its influence on the mammalian muscle nAChR over the years. Groebe *et al.* explains in previous research, α-conotoxins GI and MI tolerate a variety of side-chain substitutions in this position without significant effects on their affinity for the nAChR ([130], [128]). Referring to Table 10, there were no significant changes for the IC_{50} for mouse receptors in α-[N11A] MI, α-[K10N] SI, α-[K10H] SI and α-[H10A] GI when compared to their native sequence. Due to the following results, Groebe *et al.* believe there is no interaction between the side chain at position 10 and BC_3H-1 receptors ([126]).

However, the 4 residues found in position 10 in native α3/5 conotoxins are all polar. The side chains of these residues are also very exposed ([117]). The electrostatic potential, which is highly influenced by positions 9 and 10 in the α3/5 conotoxins, is critically important for the affinities and relative selectivity of these conotoxins on the nAChR ([117]). While Jacobsen *et al.* acknowledge the importance of position 10, the given alterations shown in Table 10 prove the residues in this position can be varied and give less of an effect on the muscle nAChR. Results of other residues that are not polar and have not been found natively in position 10 (disregarding alanine scan mutagenesis) and have yet to be tested for affinity/toxicity.

Table 10: Muscle nAChR IC_{50} readings of α3/5 conotoxin mutations at positions 4 and 10.

α-Ctx	αβδ (nM)	αβγ (μM)	αβδε (nM)	Ref.
SI	1,300 ± 430	290 ±110	-	[126]
[K10H] SI	750 ± 100	320 ± 81	-	[126]
[K10N] SI	2,100 ± 970	420 ± 89	-	[126]
MI	0.4 ± 0.1	18 ± 5	-	[117]
[H5A] MI	0.97 ± 0.44	36 ± 9	-	[117]
[N11A] MI	1.3 ± 0.1	21 ± 1	-	[117]
GI	-	-	5.86 (5.01-6.86)	[124]
[N4A] GI	-	-	4.66 (4.19-5.18)	[124]
[H10A] GI	-	-	7.62 (6.78-8.57)	[124]

Ctx, Conotoxin. This table presents three different α3/5 conotoxins with corresponding IC_{50} readings on the muscle nAChR subunits. Of the 3 toxins listed, each contains a single mutation at position 4 and/or position 10 within the α3/5 sequence. The only two substitutions that increased toxicity was [K10H] SI and [N4A] GI. All tests were done on M. musculus muscle nAChR subunits.

3.2.4 α-[P9O] ObI

YCCHPACGONFSC*

Mutation

The first analog developed (α-[P9O] ObI) is a single mutation peptide with the substitution of proline to hydroxyproline in position 9. This mutation will introduce the commonly found PTM hydroxylation of proline. A small review of the hydroxylation of proline in the introduction states that this PTM is commonly misunderstood as results vary. This analog will illustrate any potential effects from the addition of a hydroxyl group in position 9.

Position Analytics

Position 9's potential for bioengineering in the model α-ObI conotoxin sequence made way to the potential of this thesis. Proline in position 9 is not common within the α3/5 conotoxin

sequence array. However, there is a high presence of Pro-9 in α3/5 conotoxins originating from the species *C. striatus* (like α-SI). Moreover, α-conotoxin SI is also the only well-known α3/5 conotoxin that does not have a strong selectivity for αβδ subunit ([117]). Position 9 normally consists of either a lysine or an arginine for a good reason. Groebe *et al.* ([126]) explain α-SI showed comparatively minimal selectivity due to a disruption in the second disulfide loop. Rather than any specific interactions, Benie *et al.* ([120]) further explain that the surfaces being presented to nAChR binding sites of α-SI compared to α-GI/MI are electrostatically different, giving a conformational restriction via the proline ring. The addition of hydroxyproline will not revise this confirmation change. Rather, the mutation presented is strictly a test to see if the PTM proline hydroxylation will be favored.

3.2.5 α-*des*[Y] [P9O] ObI

CCHPACGONFSC*

Mutation

The second analog developed (α-*des*[Y] [P9O] ObI) is the result of a split synthesis, where the peptide was cleaved from the resin before the addition of the *N*-terminal tyrosine. The deletion mutation will represent PTM *N*-terminal truncation. This PTM also is generally misunderstood, as displayed in the introduction, but is seen throughout many native conotoxins. Ultimately, the deletion mutation will illustrate any potential side effects from the removal of an aromatic, *N*-terminal tyrosine from α-ObI.

Position Analytics

The first position in the α-ObI sequence is a tyrosine. α-SIA is the one of very few α3/5's that contain a tyrosine in position one and has nanomolar toxicity towards the αβδ subunit. Overall, residues occupying the first position are quite variable in the consensus sequence.

Previous papers have shown synthetic *N*-terminal truncation of α3/5's has little effect to the overall nAChR affinity. For example, removal of the *N*-terminal Glu-1 from α-GI or the *N*-terminal Ile-1 from α-conotoxin SI has little effect on the biological activity on the nAChR, presenting position 1 to be dispensable for function ([131],[116]). The explanation for low activity in

removal of Glu-1 from α-GI is due to how the side chain methylene groups are not represented by a strong electron density in contrast to the bulk of the toxin structure ([131]). Liu *et al.* show a reduced potency of 1.2 nM of α-Ac1.1b-ΔN (deletion the N terminus NGR) compared to α-Ac1.1b. On a side note, Liu *et al.* also explain α-Ac1.1a, α-Ac1.1b and α-Ac1.1b-ΔN failed to inhibit the nAChR when the αβδ subunit was absent, further showing the preferred specificity towards the αβδ muscle nAChR subunit ([132]). Removal of Tyr-1 from α-ObI will overall show the significance of the aromatic amino acid in the *N*-terminal.

The bioengineering of the first αα position has only seen statistically significant results in the paper by Ning *et al.* ([124]) Ning *et al.* show peptide α-[E1A] GI selectivity inhibited the mouse αβδε nAChR subunit with increased potency when compared to α-GI ([124]) (refer to Table 11). α-[E1A] GI had the highest increase of potency for the mammalian muscle nAChR on a full alanine scan mutagenesis of α-GI. It is also noted that α-[E1A] GI fully blocked acetylcholine (Ach)-evoked currents at 10 nm, while the original α-GI only blocked the Ach-evoked currents 75.5% at 10 nm ([124]). The molecular simulation showed Glu-147 in the αβδ subunit reacted with Glu-1 in the synthetic analog, producing electrostatic repulsion. When Ala-1 was replaced with Glu-1, electrostatic repulsion decreased, ultimately contributing to a stronger blockage of the αβδε nAChR ([124]).

Table 11: Muscle nAChR IC_{50} readings of α3/5 conotoxins with synthetic *N*-terminal deletion/substitution mutations.

α-Ctx	αβδ (nM)	αβδε (nM)	αβδγ (nM)	Ref.
MI	0.4 ± 0.17	-	-	[117]
[R2A] MI	1.8 ± 0.3	-	-	[117]
GI	-	5.86 (5.01-6.86)	-	[124]
[E1A] GI	-	1.83 (1.55-2.15)	-	[124]
Ac1.1b	-	-	25.8 ± 5.9	[132]
Ac1.1b -ΔN	-	-	27.0 ± 7.1	[132]

**ΔN, N-terminal truncation; Ctx, Conotoxin. The table above represents IC_{50} readings on the muscle nAChR from various α-conotoxins. α-MI and α-GI analogs show a substitution mutation, while the α-Ac1.1b analog shows a deletion mutation. All readings above were tested on M. musculus muscle nAChR subunit.*

3.2.6 α-[P9K] ObI

YCCHPACGKNFSC*

Mutation

The third analog developed is a single mutation (α-[P9K] ObI) of proline to lysine in the 9th position of the α-ObI sequence. As explained above for the first analog, position 9 is a very important position for specificity towards the muscle nAChR. This substitution will add sequence homology towards most α3/5 conotoxins and will presumably increase toxicity towards the muscle nAChR.

Position Analytics

The αα proline has a neutral charge compared to the positive charges of lysine and arginine. An analog created by Groebe *et al*. ([126]) changed Pro-9 to Lys-9, removing the conformational restriction and adding a positively charged residue to the second disulfide loop. The IC_{50} of α-[P9K] SI produced had an 870-fold increase in affinity for the αβδ in BC3H-1 mouse receptors, and 190-fold increase in affinity for the αβγ site of *Torpedo californica* receptors ([126]). This puts α-SI in the range of α-MI/GI, showing the importance of having a positively charged residue in position 9. Studies are further supported when the positively charged Arg-9 was exchanged with Ala-9 in α-GI. Results of the mutation α-[R9A] GI had a 10-fold increase in the IC_{50} for the adult nAChR αβδε ([124]). A positive charged second disulfide loop and a conserved positive charged *N*-terminus gives α-GI/MI a double positive peptide, while α-SI remains a positive/negative peptide. Lastly noted, Jacobsen *et al.* suggest the proline residue in α-SI causes the tyrosine residue in position 11 to be displaced from its optimal orientation ([117]). The importance of position 11 will be discussed further in the following sections.

Table 12: Muscle nAChR IC_{50} readings of α3/5 conotoxins with a position 9 mutation.

α-Ctx	αβδ (nM)	αβγ (μM)	αβδε (nM)	Ref.
SI	1,300 ± 430	290 ± 110	-	126
[P9K] SI	1.5 ± 0.6	70 ± 1.2	-	126
GI	-	-	5.86 (5.01-6.86)	124
[R9A] GI	-	-	49.79 (45.22-54.81)	124

Ctx, Conotoxin. The table above shows muscle nAChR IC_{50} readings of two α3/5 conotoxins and their corresponding analogs with a substitution mutation in position 9. The substitution [P9K] SI increase 870-fold increase in toxicity when compared to the native peptide. Readings above were completed on M. musculus muscle nAChR subunits.

3.2.7 α-[P9K] [F11W] ObI

YCCHPACGKNWSC*

Mutation

The fourth analog developed is the first double mutation (α-[P9K] [F11W] ObI) of Pro-9 to Lys-9 and a Phe-11 to Trp-11. Position 11, along with position 9, are among two of the most mutated positions within all α3/5 conotoxins. The purpose of substituting two different aromatic αα in position 11 was not to increase toxicity but to allow the construction of the fifth analog. However, seeing the difference in specificity will further support the importance of a bulky, aromatic residue in this position.

Position Analytics

The residue in position 11 of α-ObI is composed of phenylalanine. The position is highly conserved and consists of either tyrosine or phenylalanine in the α3/5 subfamily. Tryptophan is not found in this position in all native α3/5 conotoxins to date. Tyr-11 (Tyr-12 in α-MI) for α-GI/MI is found in a hydrophobic pocket within the mammalian muscle nAChR and interacts with

hydrophobic αα Leu-93, Tyr-95 and Leu-103 in the αβδ subunit ([118], [133], [124]). The affinity of α-MI/GI affinity between αβδ and a αβγ subunit interfaces a 10,000-fold difference, with high specificity towards the αβδ subunit. However, α-conotoxin SI is not as selective due to a micromolar affinity to mammalian muscle nAChR ([126]). Pro-9 in α-SI likely distorts the *C*-terminal loop, moving Tyr-11 out of the optimal position of its hydrophobic counterpart in the mammalian muscle nAChR binding site ([123]). This further shows the importance of polarity in the second disulfide loop.

The common similarities of the two residues found in position 11 of native α3/5 conotoxins include not only hydrophobicity but more importantly aromaticity. The combination of these two characteristics anchors the peptide onto the muscle nAChR. Substitution of Tyr-12 with the hydrophilic, non-aromatic threonine decreased affinity of α-MI 10,000-fold, whereas substitution with phenylalanine or tryptophan maintains high affinity ([123],[117]). Alanine scan mutagenesis also shows how important the aromaticity of position 11 is in α3/5 conotoxins. Referring to Table 13, alanine substitution of position 11 in α-MI changed the IC_{50} from nano to micromolar toxicities, while substitutions at positions 9 and 10 remained similar to α-MI ([117]). A similar trend is seen in alanine scan mutagenesis of α-GI with an increased IC_{50} of 5.86 nM to 381.2 nM in α-[Y11A] GI, while the substitution of alanine in positions 9 and 10 had relatively minimal change ([124]). Substitutions of position 11 in α-SI with non-aromatic αα remained unaffected with micromolar toxicities ([126]). This again highlights the negative effects Pro-9 of α-SI has on removing Tyr-11 out of its optimal position on the mammalian muscle nAChR.

Table 13: Muscle nAChR IC_{50} readings of α3/5 conotoxins with a position 11 mutation.

α-Ctx	αβδ (nM)	αβγ (μM)	αβδε (nM)	Ref.
MI	0.4 ± 0.01	18 ± 5	-	[117]
[Y12A] MI	3,400 ± 410	109 ± 15	-	[117]
[Y12M] MI	19 ± 3	10 ± 2	-	[117]
[Y12H] MI	13 ± 1	52 ± 13	-	[117]
[Y12W] MI	1.8 ± 0.2	58 ± 12	-	[117]
[Y12Y- I_2] MI	<0.4	0.04	-	[117]
GI	-	-	5.86 (5.01-6.86)	[124]
[Y11A] GI	-	-	381.2 (323.4-449.4)	[124]

[Y12Y- I_2] MI; tyrosine to diiodotyrosine substitution; Ctx, Conotoxin. The table above shows α3/5 conotoxin muscle nAChR IC_{50} readings with position 11 mutations (position 12 for α-MI). All tests were completed on M. musculus muscle nAChR subunits.

3.2.8 α-[P9K] [F11Br-W] ObI

YCCHPACGKN(Br-W)SC*

Mutation

The fifth and final analog is a double mutation (α-[P9K] [F11Br-W] ObI) of a proline to a lysine in position 9 and a phenylalanine to a bromotryptophan in position 11 of the α-ObI sequence. The specific bromination of tryptophan is a non-native L-5-bromotrytophan residue. While this substitution represents a non-native αα integration, it can also represent the PTM L-6-bromotryptophan, respectively. The original purpose of the mutation at position 11 is to increase the bulkiness of tryptophan, as seen in the iodination of tyrosine in research by Luo and McIntosh *et al.* ([134]) and Jacobsen *et al.* ([117]).

Position Analytics

Through analysis of structure-activity relationships (SAR) in alpha conotoxin α-MI, increasing the size of the hydrophobic side chain of position 12 can decrease the toxin

dissociation rate and increase potency ([117]). Jacobsen *et al*. and Luo/McIntosh *et al.* both test this idea by adding iodine to Tyr-12 in α-MI ([117], [134]). The substitution of a monoiodinated tyrosine in position 12 led to a ~20-fold increase in potency (37.8 nM to 1.66 nM) in human fetal muscle TE67 cells ([134]). Monoiodination of Tyr-12 also showed great potency and selectivity for the mouse αβδ subunit. Steric considerations of monoiodinated tyrosine face outwards from the peptide, thus extending its hydrophobic, finger-like reach. Luo and McIntosh *et al.* concluded the addition of this iodine moiety to Tyr-12 may strengthen hydrophobic interactions with key residues in the αβδ subunit ([134]). Also to note, studies show a D-tyrosine substitution in this position for α-MI and α-GI caused both to be inactive to the muscle nAChR at all concentrations tested ([130], [128]).

Through the addition of diiodotyrosine [Y12Y- I_2] MI, the iodinated analog slowed the rate of dissociation (time to wash off from receptor) when compared to the native α-MI and also increased potency at the αβγ subunit from 18 μM to 0.04 μM ([117]). Jacobsen *et al.* suggest the ability of diiodotyrosine to slow the rate of dissociation indicates the binding between this residue position and the muscle nAChR does not require a highly specific geometry (as seen in a lock-and-key model, for example) ([117]). Due to positive results of a bulky aromatic side chain of position 11 binding to a non-specific geometric, hydrophobic pocket on the receptor leads to an idea of adding non-native αα to this position to expect a possible increase in potency and reduce the dissociation rate of the peptide.

3.3 Functional Characterization of α-ObI and Analogs

3.3.1 LD_{50} : Fish Biosassy

α-ObI and the five analogs developed were administered intramuscularly into *Poecilia reticulata* to determine the LD_{50}. Fish death was recorded with every dose injection throughout the 6 peptides (disregarding the control). The overall trendline of each peptide represented a positive correlation of dose versus dose/(survival time), as seen in Figure 12. There are a few outliers observed, but the regression line remained positive.

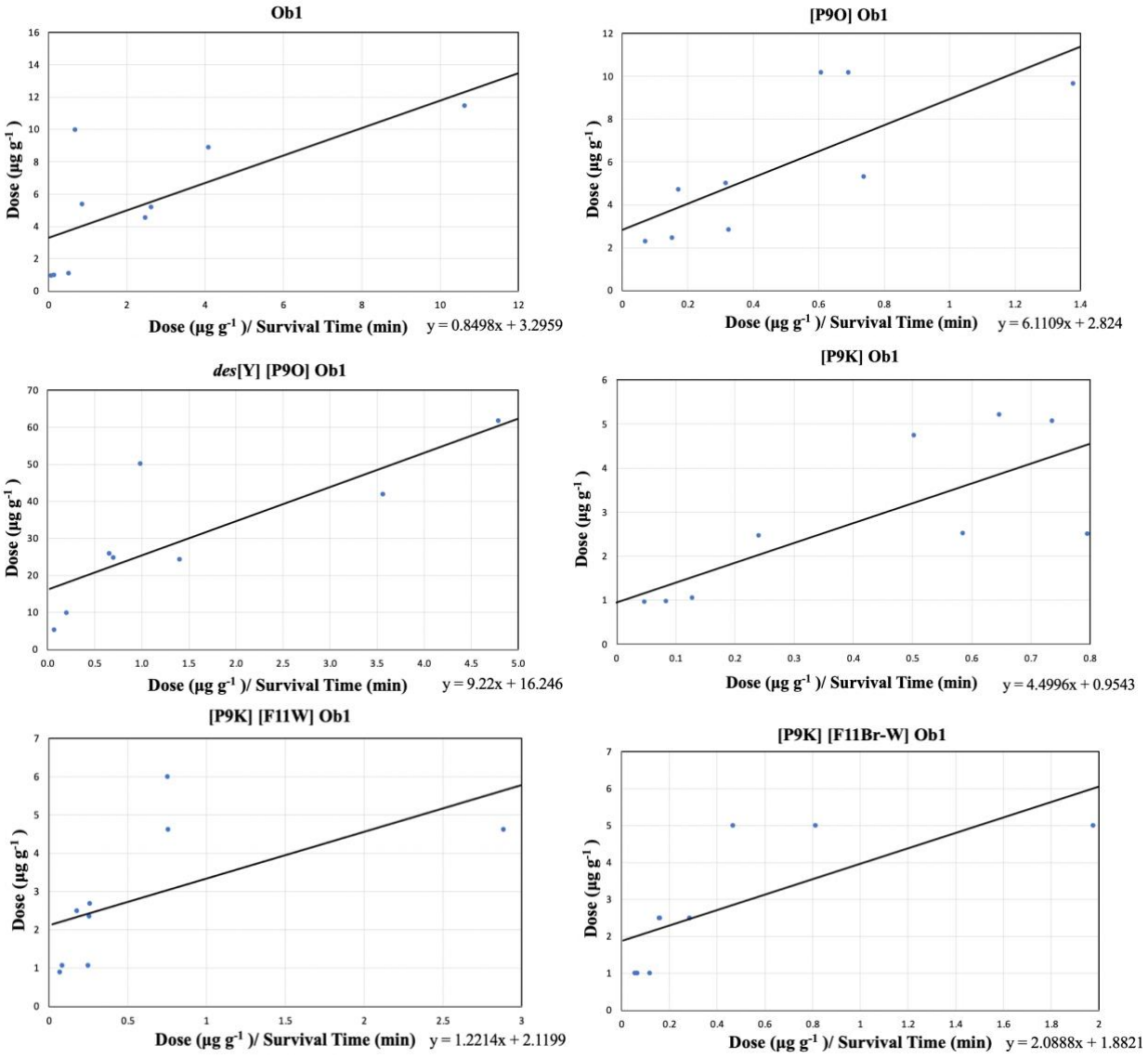

Figure 12: Fish bioassay scatterplot of dose versus dose/survival time.

The graphs above represent each fish injected in the fish bioassay experiment within α-ObI and the 5 analogs. The dose was recorded in µg g^{-1}, while survival time was recorded in minutes.

Table 14 is the LD_{50} results gathered from Figure 12. The single mutation α-[P9K] ObI produce the lowest LD_{50} value of 0.95 μg g^{-1} (0.67 nM g^{-1}), while α-*des*[Y] [P9O] ObI produced the highest LD_{50} value of 16.25 μg g^{-1} (13.00 nM g^{-1}). α-ObI and the other 3 analogs possessed relatively low LD_{50} values, falling in the range of 1.88 to 3.30 μg g^{-1} (1.22 to 2.36 nM g^{-1}).

Table 14: Fish bioassay LD_{50} readings of α-ObI plus analogs.

α-Ctx	LD_{50} (μg/g)	LD_{50} (nM/g)	Monoisotopic Mass (Da)
ObI	3.30	2.36	1,396.48
[P9O] ObI	2.82	2.00	1,412.50
des[Y] [P9O] ObI	16.25	13.00	1,249.44
[P9K] ObI	0.95	0.67	1,427.54
[P9K] [F11W] ObI	2.12	1.45	1,466.55
[P9K] [F11Br-W] ObI	1.88	1.22	1,545.45

Br-W, 5-Bromotryptophan; Ctx, Conotoxin; Da, Daltons; des[Y], N-terminal truncation; O, 4-trans-hydroxyproline. The following results shown above are the median lethal dose (LD_{50}) and the oxidized monoisotopic mass of α-ObI plus analogs. The bioassay to determine LD_{50} was completed on the species Poecilia reticulata. The LD_{50} dosage *is recorded in μg g^{-1} and nM g^{-1}.*

3.3.2 EC_{50}: *Homo sapiens* Muscle nAChR

α-ObI and 4 analogs were sent to a collaborative lab to determine the EC_{50} values. Analog α-*des*[Y] [P9O] ObI was not sent due to low yield via oxidation. In Figure 13, the following peptides exhibited 100% inhibition (disregarding α-[P9K] [F11Br-W] ObI towards the αβδϵ subunit) on a nanomolar scale of the *H. sapiens* muscle nAChR subunits: αβδ, αβγ, and αβδϵ. However, none of the following peptides possessed inhibition on a nanomolar scale towards the αβγ subunit or any of the tested *H. sapiens* neuronal nAChR subunits. This is common within most α3/5 conotoxins, with the highest specificity towards the αβδ subunit.

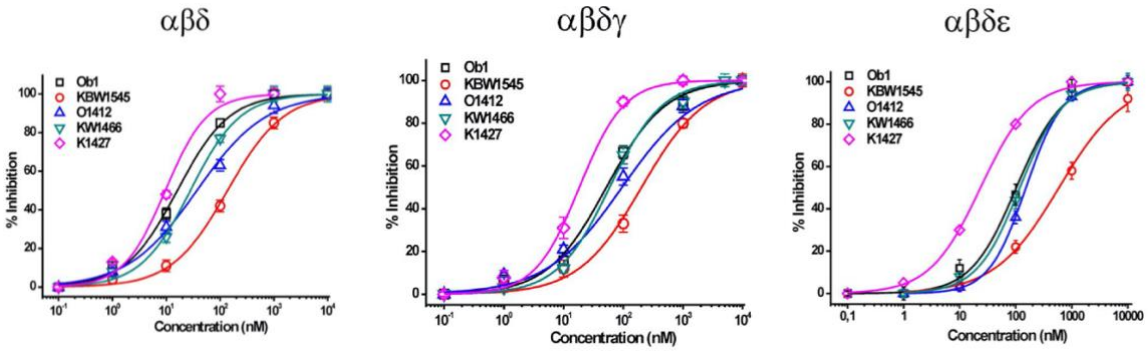

Figure 13: Percent inhibition of α-ObI plus analogs on H. sapiens muscle nAChR subunits.

The following graphs are a representation of α-ObI plus analogs percent inhibition of muscle-type nAChR subunits at a nanomolar scale. The following abbreviation is the following peptide: KBW1545 (α-[P9K] [F11Br-W] ObI), O1412 (α-[P9O] ObI), KW1466 (α-[P9K] [F11W] ObI), and K1427 (α-[P9K] ObI).

The EC_{50} was gathered from α-ObI plus analogs. According to Table 15, α-[P9K] ObI exhibited the lowest IC_{50} at 9.6 ± 1.7 nM towards the αβδ nAChR subunit, followed by the native α-ObI at 16.9 ± 1.6 nM. Although, the other 3 analogs expressed higher EC_{50}'s, with the brominated αβδ ObI analog valued at 160.7 ± 14.7 nM (~9-fold greater than αβδ ObI). EC_{50} readings of the following peptides towards the αβγ exhibited concentrations higher than 10 μM. Not enough material was available to determine the exact IC_{50} for the αβγ nAChR subunit.

The single proline substitution of α-[P9K] ObI increased the toxicity of the native peptide, as seen in the similar mutation α-[P9K] SI via Groebe *et al.* ([126]). However, replacing phenylalanine with tryptophan in α-[P9K] [F11W] ObI eliminated the effects of the proline substitution. Further elaboration will be detailed in the discussion.

Table 15: EC_{50} values of α-ObI plus analogs on the delta (δ) and gamma (γ) nAChR subunit.

α-Ctx	αβδ (nM)	αβγ (μM)
ObI	16.9 ± 1.6	>10
[P9O] ObI	37.1 ± 4.9	>10
[P9K] ObI	9.6 ± 1.7	>10
[P9K] [F11W] ObI	28.1 ± 2.9	>10
[P9K] [F11Br-W] ObI	160.7 ± 14.7	>10

Br-W, 5-Bromotryptophan; Ctx, Conotoxin; des[Y], N-terminal truncation; O, 4-trans-hydroxyproline.

EC_{50} values were also gathered towards the αβδγ and αβδϵ *H. sapiens* muscle nAChR subunits. According to Table 16, α-conotoxin ObI and analogs exhibited an overall increased EC_{50} value towards the adult nAChR subunit, demonstrating a range of 1.28 to 2.92 times higher than fetal nAChR subunits. The order of toxicity remained the same throughout αβδ, αβδγ, and αβδϵ subunits.

Table 16: EC_{50} values of α-ObI plus analogs on the fetal (αβγδ) and adult muscle (αβϵδ) nAChR subunit.

α-Conotoxin	αβδγ (nM)	αβδϵ (nM)
ObI	52.1 ± 6.6	102.8 ± 12.5
[P9O] ObI	95.3 ± 5.7	152.1 ± 2.1
[P9K] ObI	18.4 ± 1.8	23.6 ±1.2
[P9K] [F11W] ObI	59.1 ± 5.7	118.6 ±7.7
[P9K] [F11Br-W] ObI	202.5 ± 29.1	591.8 ± 50.5

Br-W, 5-Bromotryptophan; Ctx, Conotoxin; des[Y], N-terminal truncation; O, 4-trans-hydroxyproline.

Chapter 4 *Discussion*

4.1 *Conus striatus* and *Conus obscurus*

The species distribution between *C. striatus* and *C. obscurus* is found in the same general region of the Indo-Pacific. Additionally, the discovery of the novel peptide α-ObI and the well-known α-SI in *C. obscurus* milked venom presents a possibility of an evolutionary connection between the two species. This section will begin with a small introduction of α-SI and continue with multiple observations that would lead someone to believe these two cone snails may be closely related.

α-SI was originally discovered from the venom of *Conus striatus* in 1988 by Zafaralla *et al.* ([116]). This α-conotoxin has an interesting distinction from most of the α3/5 conotoxins by accompanying a proline in position 9. Groebe *et al.* ([126]) further analyzed this distinction of the proline by substituting the conserved lysine in this position, increasing the IC_{50} towards BC_3H-1 cells αβδ nAChR subunit < 800-fold . Further out, it is now understood *C. striatus* contains a substantial arsenal of α3/5 conotoxins used for prey paralysis and consumption.

Finding the same conotoxin within two different species is uncommon. α-SI discovered in the MV of *C. obscurus* is the first major element in seeing their possible evolutionary relationship. Another important element is the sequence correlation between α-ObI and the α3/5 conotoxins discovered in *C. striatus*. As you can see from the BLAST results in Table 7, out of the top 5 highest BLAST scores, 4 out of the 5 conotoxins originated via *C. striatus.*

There are two distinct αα correlations between α-ObI and the *C. striatus* α-3/5 conotoxins. This first is the proline in position 9. Out of the discovered α3/5 conotoxins, the following α-conotoxins has a proline in this position; α-SI/S1.8 (*C. striatus*), α-Sm1.1 (*C. stercusmuscarum*), and α-Ci1.3 (*C. circumcisus*). According to Espiritu *et al*., these three species mentioned have a 97% likelihood of belonging to the same clade based upon their mitochondrial 16s ribosomal sequence. It is also reported that *C. obscurus* belongs to a different clade within

the fish-hunting species, but is identified as weakly supported ([135]). The biological significance of this proline is generally misunderstood due to the negative effects it has in ion peptide/receptor specificity, as shown in Groebe *et al.* ([126]). However, α-SI and α-ObI does kill fish at low concentrations and may be the explanation on why this proline has been present in multiple *Conus* species.

The second αα correlation between these two species is the tyrosine found in the *N*-terminal in α-SIA/S1.8/1.9/1.10 (*C. striatus*) and α-ObI. These 5 peptides are not only the only α3/5 conotoxins to contain a tyrosine in this position, but also the only five to have an aromatic αα in the *N*-terminal. Aromatic αα have many implications in peptide/receptor structure-activity relationships due to the bulky size of the aromatic ring. The function of the aromatic αα in the *N*-terminal is unknown. However, the removal of the tyrosine from the *N*-terminal of α-ObI decreased potency towards fish. This highlights the importance of the tyrosine in this position.

Determining an evolutionary relationship based upon mature conotoxin sequences is an attractive venture. However, it has not been proven to be an accurate source to determine the phylogeny of *Conus*. The further interpretation would be needed to fully examine the evolutionary relationship between these two species.

4.2 α-[P9O] ObI, α-des[Y] [P9O] ObI, and α-[P9K] ObI: Single Mutated Analogs

The substitution of a hydroxylated proline into the α-ObI sequence (α-[P9O] ObI) was the first PTM introduced into analog development. Inclusion of this prevalent PTM was due to certain α4/7 (α-EI, α-SrIA, and α-SrIB) and α4/4 (α-EIIA, α-EIIB, and α-PIB) conotoxins containing a hydroxyproline with muscle nAChR affinity, as well as hydroxyproline discovery in α3/5 [Hyp-4] CnID and [Hyp-7] CnIK conotoxins via MS-MS data with no tested functional characterization (see Table 17) ([136]). α4/7 and α4/4 conotoxins generally have a high affinity towards the neuronal nAChR. However, most α4/7 and α4/4 conotoxins that contain hydroxyproline have muscle nAChR affinity. Although, α4/7 SrIA/B both contain the tyrosine in

the second disulfide loop and α-EI contains the conserved histidine and proline in the first disulfide loop. In α4/4, α-EIIA, α-EIIB, and α-PIB contain the conserved H/NPA in the first disulfide loop. These characteristics mentioned (underlined in Table 17) are homologous to α3/5 conotoxins and may contribute to muscle nAChR specificity rather than the presence of hydroxyproline ([137],[138]). Overall, hydroxyproline has been observed in α-conotoxins with muscle nAChR affinity. Whether this has biological relevance or function is unknown.

Table 17: Comparison in α-conotoxins that contain an hydroxyproline and have muscle nAChR specificity.

α-Conotoxin	N/S	Loop Size	Sequence	Target	PA (nM)	Organism	Ref.
[P9O] ObI	S	3/5	Y**C**C**C**HPA**C**GONFS**C***	αβδ	37.1 ± 4.9	*Homo sapiens*	This work
[Hyp-4] CnID	N	3/5	**C**C**C**HOA**C**GKHFN**C***	ND	ND	ND	[136]
[Hyp-7] CnIK	N	3/5	NGR**C**C**C**HOA**C**GKYYS**C***	ND	ND	ND	[136]
EIIA	N	4/4	ZTOG**C**C**C**WNPA**C**VKNR**C***	αβγδ	0.46 ± 0.15	*Torpedo marmorata*	[139]
EIIB	N	4/4	ZTOG**C**C**C**WHPA**C**GKNR**C***	αβγδ	2.2 ± 0.7	*Torpedo marmorata*	[140]
PIB	N	4/4	ZSOG**C**C**C**WNPA**C**VKNR**C***	αβϵδ	36	*Mus musculus*	[137]
EI	N	4/7	RDO**C**C**C**YHPT**C**NMSNPQI**C***	αβϵδ	65.9 ± 15.7	*Mus musculus*	[141]
[O3A] EI	S	4/7	RDA**C**C**C**YHPT**C**NMSNPQI**C***	αβϵδ	104 ± 28	*Mus musculus*	[141]
SrIA	N	4/7	RT**C**C**C**SROT**C**RMγYPγL**C**G*	αβγδ	NF	*Homo sapiens*	[137]
SrIB	N	4/7	RT**C**C**C**SROT**C**RMEYPγL**C**G*	αβγδ	NF	*Homo sapiens*	[137]
[γ15E] SrIB	S	4/7	RT**C**C**C**SROT**C**RMEYPEL**C**G*	αβγδ	1.8 ± 1.9	*Homo sapiens*	[137]
Vc1A	N	4/7	G**C**C**C**SDOR**C**NYDHPγI**C***	αβγδ	NA	*Rattus norvegicus*	[142]
[P9O] Vc1.1	S	4/7	G**C**C**C**SDOR**C**NYDHPEI**C***	αβγδ	NA	*Rattus norvegicus*	[142]
GID	N	4/7	IRDγ**C**C**C**SNPA**C**RVNNOHV**C***	αβγδ	NA	*Rattus norvegicus*	[143]
ArIA	N	4/7	IRDE**C**C**C**SNPA**C**RVNNOHV**C**RRR*	αβγδ	NA	*Rattus norvegicus*	[144]

**, C-terminal amidation; O/Hyp,4-trans-hydroxyproline; Z, pyroglutamic acid; γ,γ-carboxyglutamate; N, native; S, synthetic construct; NA, not active; ND, not determined; NF, not finalized; PA, pharmacological activity. Comparison between α-[P9O] ObI and α3/5, α4/4, and α4/7 sequences with muscle nAChR specificity that contain hydroxyproline. The cysteines are in bold, hydroxyprolines are highlighted in red, and homologous αα in relation to α3/5 conotoxins are underlined.*

The addition of the hydroxyl group in α-[P9O] ObI retained low LD_{50} in fish, but increased the EC_{50} ~2-fold towards the αβδ and αβδγ subunits when compared to the native α-ObI. A common characteristic of α3/5, α4/7, and α4/4 show the presence of the hydroxyproline in the *N*-terminal or first disulfide loop. However, the PTM in α-[P9O] ObI is presented in the second disulfide loop. Considering the native α3/5 conotoxins, α-[Hyp-4] CnID and α-[Hyp-7] CnIK with hydroxyproline found in the first disulfide loop, a hydroxyproline substitution with the proline found in the first disulfide loop of α-ObI should be looked into. All in all, the PTM substitution in α-[P9O] ObI did retain nanomolar EC_{50} towards the neuromuscular nAChR and killed fish at all tested doses.

The second PTM introduced, *N*-terminal truncation, was observed in α-*des*[Y] [P9O] ObI. Truncated peptides present a more drug-like appearance with an economic advantage towards producing novel therapeutics ([96]). Although, there have been little to no cases of decreased IC_{50} from a synthetic deletion of the entire *N*-terminal in α3/5 conotoxins. Previous research has been unsuccessful in determining the purpose of *N*-terminal deletion in native peptides. Although, there are multiple examples of α3/5 *N*-terminal deletion found in nature; α-MIC (*C. magus*) ([97]), α-des-Ile-SI (*C. striatus*) ([116]), α-CnIB/C/D/E/G (*C. consors*) ([136]).

The analog α-*des*[Y] [P9O] ObI overall produced a low yield after both oxidations. Only enough peptide was available for the fish bioassay. The overall LD_{50} of the truncated analog was 13.00 nM g^{-1}, while the other analogs plus α-ObI fell in the range of 0.67 to 2.36 nM g^{-1}. Considering a much higher dose (> 2.5μg g^{-1}) was needed to cause fish death, repeating another synthesis of α-*des*[Y] [P9O] ObI was not concluded.

α-[P9K] ObI was introduced because of the positive effects of the lysine in this position shown in past research. Groebe *et al.* ([126]) changed Pro-9 to Lys-9 in α-SI , producing an 870-fold increase in affinity for the αβδ subunit in BC3H-1 receptors, and 190-fold increase in affinity for the αβγ subunit of *Torpedo californica* receptors. Groebe *et al.* suggested there is an imbalance of charge, which attributes to the lowered toxicity. Proline in α-SI makes the *C*-terminal negatively charged, while the *N*-terminal end is positively charged. When the proline is replaced with a lysine, this will cause a positive *N*/*C*-terminal, relating the peptide to the other

highly toxic α3/5 conotoxins . However, Jacobsen *et al.* ([117]) does not agree with Groebe, stating the proline in α-SI rather displaces the tyrosine in the second disulfide loop out of its optimal position. However, this proline is seen to be passed down throughout the *Conus* genus and ultimately increases the peptide diversity of α3/5 conotoxins.

α-[P9K] ObI was the only analog that overall decreased the EC_{50} of *H. sapiens* muscle nAChR; ~2-fold in αβδ, ~3-fold in αβδγ, and ~4-fold in αβδϵ subunits. α-[P9K] ObI also had the lowest LD_{50} characterization at 0.67 nM g^{-1}. This is the second example of a proline to lysine substitution increasing the toxicity of the α3/5, as seen in α-[P9K] SI. Ultimately, α-[P9K] ObI favors the suggestion of the negative effect proline may have in this position towards the mammalian muscle nAChRs.

4.3 α-[P9K] [F11W] ObI & α-[P9K] [F11Br-W] ObI: Double Mutated Analogs

α-[P9K] [F11W] ObI retains the lysine in position 9 and substitutes the aromatic αα's phenylalanine to tryptophan. Due to past research, the tryptophan substitution was presumed to have little to no effect on the overall EC_{50} to the mammalian muscle nAChR or fish lethality. The only synthetic tryptophan substitution in α3/5 conotoxins was completed via Jacobsen *et al.*. The substitution α-[Y12W] MI maintained high affinity towards the αβδ mouse muscle nAChR subunit, only increasing IC_{50} from 0.40 ± 0.17 nM to 1.5 ± 0.2 nM ([117]). However, tryptophan has not been found in position 11 in all native α3/5 conotoxins.

α-[P9K] [F11W] ObI EC_{50} results proved my assumption incorrect, as changing an aromatic αα within this position had a comparatively significant increase towards the *H. sapiens* muscle nAChR. The EC_{50} increased ~3-fold towards αβδ/αβδγ and ~5-fold towards αβδϵ subunits, when compared to α-[P9K] ObI. In other words, the phenylalanine to tryptophan substitution eliminated the positive effects of the lysine in position 9 towards the *H. sapiens* muscle nAChR. α-[P9K] [F11W] ObI ended up having a higher EC_{50} than the native α-ObI peptide in the αβδ, αβδγ, and αβδϵ subunits, but did have increased toxicity in fish.

As you can see from Table 18, α-[Y12W] MI had a 1.1 nM (~4-fold) IC_{50} increase to α-MI and considered overall no significant change in potency ([117]). Since α-[P9K] ObI had a higher relative concentration, the EC_{50} comparison of α-[P9K] ObI and α-[P9K] [F11W] ObI is comparatively significant at an 18.5 nM increase, even if we had a lower ~3-fold EC_{50} increase. Past research indicates position 11's aromaticity, hydrophobicity, and bulkiness anchor the peptide into the hydrophobic pocket presented in the muscle nAChR. Tryptophan is the largest αα, contains an aromatic ring, and is hydrophobic. However, tryptophan's chemical structure contains an indole ring (bicyclic ring composed of one benzene and pyrrole group) which adds to the αα high hydrophobicity. Although, tyrosine and phenylalanine only contain one benzene ring. The contrasting structure of tryptophan's pyrrole group may disrupt peptide/receptor binding, thus affecting the EC_{50} of α-[P9K] [F11W] ObI towards muscle nAChR. Our research highlights position 11's geometric structure has a high importance mammalian muscle nAChR affinity and could be the reason behind the absence of tryptophan in this position.

Table 18: Tryptophan substitution in α3/5 conotoxins.

α-Ctx	N/S	Loop Size	Sequence	Target	PA (nM)	Organism	Ref.
[P9K] ObI	S	3/5	Y**CC**HPA**C**GKNFS**C***	αβδ	9.6 ± 1.7	*Homo sapiens*	This work
[P9K] [F11W] ObI	S	3/5	Y**CC**HPA**C**GKNWS**C***	αβδ	28.1 ± 2.9	*Homo sapiens*	This work
MI	N	3/5	GR**CC**HPA**C**GKNYS**C***	αβδ	0.40 ± 0.17	*Mus musculus*	[117]
[Y12W] MI	S	3/5	GR**CC**HPA**C**GKNWS**C***	αβδ	1.5 ± 0.2	*Mus musculus*	[117]

**, C-terminal amidation; Ctx, Conotoxin; N, native; S, synthetic construct; PA, pharmacological activity. Comparison in pharmacological activity of tryptophan substitution in α-MI and α-ObI. The cysteines are in bold, and the position of mutation is in red.*

The last PTM tested was the bromination of tryptophan, represented in the double mutated analog α-[P9K] [F11Br-W] ObI. L-6-bromotryptophan is found natively throughout *Conus* venom, and the overall purpose of this PTM in nature is generally misunderstood. The αα added to position 11 in α-ObI was L-5-bromotryptophan. Bromotrytophan introduction into α-ObI was selected due to the increased toxicity recorded by the addition of monoiodination and diiodonation of tyrosine in α-MI by Luo *et al.* ([134]) and Jacobsen *et al.* ([117]). Luo *et al.* suggested the addition of the single iodine to tyrosine in position 12 may strengthen hydrophobic interactions with key residues in the αβδ subunit. Jacobsen *et al.* suggested by the addition of diiodine to tyrosine in position 12, the increase in toxicity showed a rather nonspecific hydrophobic interaction could be involved between the conotoxin and δ receptor interface. Due to the high favorability of a bulky, hydrophobic αα in this position, the addition of L-5-bromotryptophan in α-ObI allowed us to see any effects of halogen and non-native αα integration, as well as the PTM bromination of tryptophan respectively.

α-[P9K] [F11Br-W] ObI had the highest EC_{50} (overall nanomolar affinity still observed) out of all the peptides tested towards αβδ, αβδγ, and αβδϵ *H. sapiens* muscle nAChR subunits. This result is most likely due to the negative effects of tryptophan in this position (as shown in α-[P9K] [F11W] ObI) and re-iterates the importance of αα geometry in position 11 for peptide/receptor affinity towards the mammalian muscle nAChR. However, α-[P9K] [F11Br-W] ObI had the second-lowest LD_{50} reading at 1.22 nM g^{-1} in the fish bioassay.

The PTM bromination of tryptophan may have evolved into *Conus* venom based on its high potency to marine organisms rather than the mammalian muscle nAChR. There is no shortage of bromine in marine environments as it is a common element found in seawater. Brominated compounds have not only been frequently seen in *Conus* but also in sessile marine organisms that use brominated compounds as metabolites for predator defense ([145]). Further research and interpretation would be needed to confirm this hypothesis.

4.4 Future Work and Closing

The following research intended purpose pertained to native sequence discovery via MS analysis, implementing fmoc-SPPS peptide synthesis, utilizing synthetic PTM integration, and analyzing functional characterization (LD_{50} and EC_{50}) of native/synthetic peptides originating from *C. obscurus*.

Future work to continue off of this thesis includes a further examination of any additional α3/5 mature conotoxin sequences, as well as genetic information existing in the milked venom of *C. obscurus*, would be needed to provide more evidence of a possible close evolutionary relationship between *C. striatus* and *C. obscurus.* Also, NMR and computer programming methods to analyze peptide/receptor modeling will resolve the possible effects of the 3 PTMs analyzed, the aromatic αα in the *N*-terminal, and the tryptophan (as compared to phenylalanine or tyrosine) in position 11 of α-ObI. Lastly, to create a synthetic construct with a hydroxyproline in the first disulfide loop of α-ObI to confirm or deny some suspicions of α-conotoxins containing hydroxyproline with muscle nAChR affinity.

The hypothesis of this thesis is α-ObI can be mutated to increase overall potency towards the muscle-type nAChR, as well as incorporate PTMs to ultimately investigate the boundaries of peptide bioengineering in the generation of novel α-conotoxins. The hypothesis is accurate from the many discoveries in this research in the order as follows: (i) Confirmed a novel, active sequence via MS from the MV of *C. obscurus* and gave it the name α-ObI. (ii) Discovered the presumed α-SI within the MV of *C. obscurus* and uncovered a possible close evolutionary relationship via mature conotoxin sequences of *C. striatus* and *C. obscurus*. (iii) Developed five synthetic constructs from α-ObI with nanomolar affinity to fish and four with nanomolar affinity to *H. sapiens* muscle nAChR. (iv) Confirmed α-[P9K] ObI increased potency in fish and *H. sapiens* muscle nAChR when compared to the native α-ObI. (v) Successfully incorporated 3 misunderstood PTMs commonly found in *Conus* venom into the α-ObI sequence. (vi) Lastly, we confirmed and questioned the past structure-activity relationship with α3/5 conotoxins and the muscle nAChR. The main drive of this thesis was to ultimately push the boundaries of what is

possible within the α3/5 conotoxin framework and expand the drive for peptide engineering in pharmaceutical research and development.

References

1. Lee, A. C.-L., Harris, J. L., Khanna, K. K. & Hong, J.-H. A Comprehensive Review on Current Advances in Peptide Drug Development and Design. *Int. J. Mol. Sci.* **20**, (2019).
2. The growing significance of peptide therapeutics. https://www.gesundheitsindustrie-bw.de/en/article/news/the-growing-significance-of-peptide-therapeutics.
3. Vlieghe, P., Lisowski, V., Martinez, J. & Khrestchatisky, M. Synthetic therapeutic peptides: science and market. *Drug Discov. Today* **15**, 40–56 (2010).
4. Uhlig, T. *et al.* The emergence of peptides in the pharmaceutical business: From exploration to exploitation. *EuPA Open Proteomics* **4**, 58–69 (2014).
5. Lau, J. L. & Dunn, M. K. Therapeutic peptides: Historical perspectives, current development trends, and future directions. *Bioorg. Med. Chem.* **26**, 2700–2707 (2018).
6. Pennington, M. W., Czerwinski, A. & Norton, R. S. Peptide therapeutics from venom: Current status and potential. *Bioorg. Med. Chem.* **26**, 2738–2758 (2018).
7. Bhattacharyya, D. Therapeutic Use of Snake Venom Components: A Voyage from Ancient to Modern India. *Mini-Rev. Org. Chem.* **11**, 45–54 (2014).
8. Harvey, A. L. Toxins and drug discovery. *Toxicon Off. J. Int. Soc. Toxinology* **92**, 193–200 (2014).
9. Kaas, Q. & Craik, D. J. Bioinformatics-Aided Venomics. *Toxins* **7**, 2159–2187 (2015).
10. Davis, J., Jones, A. & Lewis, R. J. Remarkable inter- and intra-species complexity of conotoxins revealed by LC/MS. *Peptides* **30**, 1222–1227 (2009).

11. Duda, T. F., Kohn, A. J. & Matheny, A. M. Cryptic Species Differentiated in Conus ebraeus, a Widespread Tropical Marine Gastropod. *Biol. Bull.* **217**, 292–305 (2009).

12. Puillandre, N. *et al.* Molecular phylogeny and evolution of the cone snails (Gastropoda, Conoidea). *Mol. Phylogenet. Evol.* **78**, 290–303 (2014).

13. Vidal, N. *et al.* The phylogeny and classification of caenophidian snakes inferred from seven nuclear protein-coding genes. *C. R. Biol.* **330**, 182–187 (2007).

14. Cao, Z. *et al.* The genome of Mesobuthus martensii reveals a unique adaptation model of arthropods. *Nat. Commun.* **4**, 1–10 (2013).

15. Peng, L. & Jackson, D. R. Circular-polarized compact low-profile omni-directional antenna. in *2013 IEEE Antennas and Propagation Society International Symposium (APSURSI)* 1472–1473 (2013). doi:10.1109/APS.2013.6711395.

16. Mm, B. Spider venom: An insecticide whose time has come? Bioinsecticide maker Vestaron says fruit and vegetable farmers are ready for its spider venom peptide. *Chem. Eng. News* **95**, 30–31 (2017).

17. Herzig, V. & King, G. F. The Cystine Knot Is Responsible for the Exceptional Stability of the Insecticidal Spider Toxin ω-Hexatoxin-Hv1a. *Toxins* **7**, 4366–4380 (2015).

18. Cushman, D. W., Cheung, H. S., Sabo, E. F. & Ondetti, M. A. Design of potent competitive inhibitors of angiotensin-converting enzyme. Carboxyalkanoyl and mercaptoalkanoyl amino acids. *Biochemistry* **16**, 5484–5491 (1977).

19. Van de Werf, F. Clinical trials with glycoprotein IIb/IIIa receptor antagonists in acute coronary syndromes. *Thromb. Haemost.* **78**, 210–213 (1997).

20. Bell, W. R. Defibrinogenating enzymes. *Drugs* **54 Suppl 3**, 18–30; discussion 30-31 (1997).

21. Pennington, M. W. *et al.* Development of Highly Selective Kv1.3-Blocking Peptides Based on the Sea Anemone Peptide ShK. *Mar. Drugs* **13**, 529–542 (2015).

22. Dardevet, L. *et al.* Chlorotoxin: A Helpful Natural Scorpion Peptide to Diagnose Glioma and Fight Tumor Invasion. *Toxins* **7**, 1079–1101 (2015).

23. Shah, A. C., Genoni, M., Niederhäuser, U., Maloigne, M. & Turina, M. [R-hirudin (lepirudin, refludan) as an alternative anticoagulant in heparin-induced thrombocytopenia during cardiopulmonary bypass connection]. *Schweiz. Med. Wochenschr.* **130**, 896–899 (2000).

24. Maraganore, J. M., Bourdon, P., Jablonski, J., Ramachandran, K. L. & Fenton, J. W. Design and characterization of hirulogs: a novel class of bivalent peptide inhibitors of thrombin. *Biochemistry* **29**, 7095–7101 (1990).

25. Miljanich, G. P. Ziconotide: neuronal calcium channel blocker for treating severe chronic pain. *Curr. Med. Chem.* **11**, 3029–3040 (2004).

26. Teichert, R. W., Jimenez, E. C. & Olivera, B. M. 36 - Biology and Pharmacology of Conotoxins. in *Botulinum Toxin* (eds. Jankovic, J. et al.) 446–464 (W.B. Saunders, 2009). doi:10.1016/B978-1-4160-4928-9.00036-6.

27. Lewis, R. J. Case Study 1: Development of the analgesic drugs prialt and Xen2174 from cone snail venoms. *RSC Drug Discov. Ser.* **2015**, 245–254 (2015).

28. Castellino, F. J. & Prorok, M. Conantokins: inhibitors of ion flow through the N-methyl-D-aspartate receptor channels. *Curr. Drug Targets* **1**, 219–235 (2000).

29. Sang, C. N., Barnabe, K. J. & Kern, S. E. Phase IA Clinical Trial Evaluating the Tolerability, Pharmacokinetics, and Analgesic Efficacy of an Intrathecally Administered Neurotensin A Analogue in Central Neuropathic Pain Following Spinal Cord Injury. *Clin. Pharmacol. Drug Dev.* **5**, 250–258 (2016).

30. Olivera, B. M. *et al.* Diversity of Conus Neuropeptides. *Science* **249**, 257–263 (1990).

31. Norton, R. S. Peptide Toxin Structure and Function by NMR. in *Modern Magnetic Resonance* (ed. Webb, G. A.) 1–18 (Springer International Publishing, 2017). doi:10.1007/978-3-319-28275-6_120-1.

32. Prashanth, J. R., Lewis, R. J. & Dutertre, S. Towards an integrated venomics approach for accelerated conopeptide discovery. *Toxicon* **60**, 470–477 (2012).

33. Fu, Y. *et al.* Discovery Methodology of Novel Conotoxins from Conus Species. *Mar. Drugs* **16**, (2018).

34. Bingham, J.-P., Mitsunaga, E. & Bergeron, Z. L. Drugs from slugs—Past, present and future perspectives of ω-conotoxin research. *Chem. Biol. Interact.* **183**, 1–18 (2010).

35. Kumar, P. S., Kumar, D. S. & Umamaheswari, S. A perspective on toxicology of Conus venom peptides. *Asian Pac. J. Trop. Med.* **8**, 337–351 (2015).

36. Akondi, K. B. *et al.* Discovery, Synthesis, and Structure–Activity Relationships of Conotoxins. *Chem. Rev.* **114**, 5815–5847 (2014).

37. Prashanth, J. R. *et al.* The role of defensive ecological interactions in the evolution of conotoxins. *Mol. Ecol.* **25**, 598–615 (2016).

38. Jin, A.-H. *et al.* Conotoxins: Chemistry and Biology. *Chem. Rev.* (2019) doi:10.1021/acs.chemrev.9b00207.

39. Schulz, J. R., Jan, I., Sangha, G. & Azizi, E. The high speed radular prey strike of a fish-hunting cone snail. *Curr. Biol.* **29**, R788–R789 (2019).

40. Venom kinematics during prey capture in Conus: the biomechanics of a rapid injection system | Journal of Experimental Biology. https://jeb.biologists.org/content/213/5/673.

41. McIntosh, M., Cruz, L. J., Hunkapiller, M. W., Gray, W. R. & Olivera, B. M. Isolation and structure of a peptide toxin from the marine snail Conus magus. *Arch. Biochem. Biophys.* **218**, 329–334 (1982).

42. Hermitte, L. C. D. Venomous marine molluscs of the genus conus. *Trans. R. Soc. Trop. Med. Hyg.* **39**, 485–512 (1946).

43. Cruz, L. J., White, J. & White, J. Clinical Toxicology of Conus Snail Stings. *Handbook of Clinical Toxicology of Animal Venoms and Poisons* https://www.taylorfrancis.com/ (2017) doi:10.1201/9780203719442-9.

44. McIntosh, J. M. & Jones, R. M. Cone venom–from accidental stings to deliberate injection. *Toxicon* **39**, 1447–1451 (2001).

45. Han, T. S., Teichert, R. W. & Bulaj, B. M. O. and G. Conus Venoms - A Rich Source of Peptide-Based Therapeutics. *Current Pharmaceutical Design* http://www.eurekaselect.com/67669/article (2008).

46. Gray, W. R., Luque, A., Olivera, B. M., Barrett, J. & Cruz, L. J. Peptide toxins from Conus geographus venom. *J. Biol. Chem.* **256**, 4734–4740 (1981).

47. Fainzilber, M. *et al.* γ-Conotoxin-PnVIIA, A γ-Carboxyglutamate-Containing Peptide Agonist of Neuronal Pacemaker Cation Currents. *Biochemistry* **37**, 1470–1477 (1998).

48. Fainzilber, M., Gordon, D., Hasson, A., Spira, M. E. & Zlotkin, E. Mollusc-specific toxins from the venom of Conus textile neovicarius. *Eur. J. Biochem.* **202**, 589–595 (1991).

49. Rigby, A. C. *et al.* A conotoxin from Conus textile with unusual posttranslational modifications reduces presynaptic Ca2+ influx. *Proc. Natl. Acad. Sci.* **96**, 5758–5763 (1999).

50. Buczek, O. *et al.* Structure and Sodium Channel Activity of an Excitatory I1-Superfamily Conotoxin,. *Biochemistry* **46**, 9929–9940 (2007).

51. Terlau, H. *et al.* Strategy for rapid immobilization of prey by a fish-hunting marine snail. *Nature* **381**, 148–151 (1996).

52. Cruz, L. J. *et al.* Conus geographus toxins that discriminate between neuronal and muscle sodium channels. *J. Biol. Chem.* **260**, 9280–9288 (1985).

53. Sharpe, I. A. *et al.* Two new classes of conopeptides inhibit the α1-adrenoceptor and noradrenaline transporter. *Nat. Neurosci.* **4**, 902–907 (2001).

54. England, L. J. *et al.* Inactivation of a Serotonin-Gated Ion Channel by a Polypeptide Toxin from Marine Snails. *Science* **281**, 575–578 (1998).

55. Petrel, C. *et al.* Identification, structural and pharmacological characterization of τ-CnVA, a conopeptide that selectively interacts with somatostatin sst3 receptor. *Biochem. Pharmacol.* **85**, 1663–1671 (2013).

56. Kerr, L. M. & Yoshikami, D. A venom peptide with a novel presynaptic blocking action. *Nature* **308**, 282–284 (1984).

57. Morales Duque, H., Campos Dias, S. & Franco, O. L. Structural and Functional Analyses of Cone Snail Toxins. *Mar. Drugs* **17**, 370 (2019).

58. Dutertre, S., Nicke, A. & Tsetlin, V. I. Nicotinic acetylcholine receptor inhibitors derived from snake and snail venoms. *Neuropharmacology* **127**, 196–223 (2017).

59. Terlau, H. & Olivera, B. M. Conus venoms: a rich source of novel ion channel-targeted peptides. *Physiol. Rev.* **84**, 41–68 (2004).

60. Kaas, Q., Westermann, J.-C. & Craik, D. J. Conopeptide characterization and classifications: An analysis using ConoServer. *Toxicon* **55**, 1491–1509 (2010).

61. Conus Venom Peptide Pharmacology | Pharmacological Reviews. http://pharmrev.aspetjournals.org.eres.library.manoa.hawaii.edu/content/64/2/259.

62. Espiritu, M. J., Cabalteja, C. C., Sugai, C. K. & Bingham, J.-P. Incorporation of post-translational modified amino acids as an approach to increase both chemical and biological diversity of conotoxins and conopeptides. *Amino Acids* **46**, 125–151 (2014).

63. Marshall, I. G. & Harvey, A. L. Selective neuromuscular blocking properties of α-conotoxins In vivo. *Toxicon* **28**, 231–234 (1990).

64. Muttenthaler, M., B. Akondi, K. & F. Alewood, P. Structure-Activity Studies on Alpha-Conotoxins. *Curr. Pharm. Des.* **17**, 4226–4241 (2011).

65. Bingham, J.-P., Andrews, E. A., Kiyabu, S. M. & Cabalteja, C. C. Drugs from Slugs. Part II – Conopeptide bioengineering. *Chem. Biol. Interact.* **200**, 92–113 (2012).

66. Nicke, A., Wonnacott, S. & Lewis, R. J. α-Conotoxins as tools for the elucidation of structure and function of neuronal nicotinic acetylcholine receptor subtypes. *Eur. J. Biochem.* **271**, 2305–2319 (2004).

67. Gotti, C. & Clementi, F. Neuronal nicotinic receptors: from structure to pathology. *Prog. Neurobiol.* **74**, 363–396 (2004).

68. Unwin, N. Refined Structure of the Nicotinic Acetylcholine Receptor at 4 Å Resolution. *J. Mol. Biol.* **346**, 967–989 (2005).

69. Romanelli, M. N. *et al.* Central Nicotinic Receptors: Structure, Function, Ligands, and Therapeutic Potential. *ChemMedChem* **2**, 746–767 (2007).

70. Buczek, O., Bulaj, G. & Olivera, B. M. Conotoxins and the posttranslational modification of secreted gene products. *Cell. Mol. Life Sci.* **62**, 3067–3079 (2005).

71. Larsen, M. R., Trelle, M. B., Thingholm, T. E. & Jensen, O. N. Analysis of posttranslational modifications of proteins by tandem mass spectrometry. *BioTechniques* **40**, 790–798 (2006).

72. Woodward, S. R., Cruz, L. J., Olivera, B. M. & Hillyard, D. R. Constant and hypervariable regions in conotoxin propeptides. *EMBO J.* **9**, 1015–1020 (1990).

73. Nair, S. S. *et al.* De Novo Sequencing and Disulfide Mapping of a Bromotryptophan-Containing Conotoxin by Fourier Transform Ion Cyclotron Resonance Mass Spectrometry. *Anal. Chem.* **78**, 8082–8088 (2006).

74. Kaas, Q., Yu, R., Jin, A.-H., Dutertre, S. & Craik, D. J. ConoServer: updated content, knowledge, and discovery tools in the conopeptide database. *Nucleic Acids Res.* **40**, D325–D330 (2012).

75. Price-Carter, M., Gray, W. R. & Goldenberg, D. P. Folding of omega-conotoxins. 2. Influence of precursor sequences and protein disulfide isomerase. *Biochemistry* **35**, 15547–15557 (1996).

76. Bingham, J.-P. *et al.* Optimizing the connectivity in disulfide-rich peptides: alpha-conotoxin SII as a case study. *Anal. Biochem.* **338**, 48–61 (2005).

77. Kang, T. S., Vivekanandan, S., Jois, S. D. S. & Kini, R. M. Effect of C-Terminal Amidation on Folding and Disulfide-Pairing of α-Conotoxin ImI. *Angew. Chem. Int. Ed.* **44**, 6333–6337 (2005).

78. Wen, J. & Hung, A. Effects of C-Terminal Carboxylation on α-Conotoxin LsIA Interactions with Human α7 Nicotinic Acetylcholine Receptor: Molecular Simulation Studies. *Mar. Drugs* **17**, (2019).

79. Khoo, K. K. *et al.* Structure of the analgesic mu-conotoxin KIIIA and effects on the structure and function of disulfide deletion. *Biochemistry* **48**, 1210–1219 (2009).

80. Flinn, J. P. *et al.* Role of disulfide bridges in the folding, structure and biological activity of omega-conotoxin GVIA. *Biochim. Biophys. Acta* **1434**, 177–190 (1999).

81. Gowd, K. H. *et al.* Dissecting a role of evolutionary-conserved but noncritical disulfide bridges in cysteine-rich peptides using ω-conotoxin GVIA and its selenocysteine analogs. *Pept. Sci.* **98**, 212–223 (2012).

82. Dutton, J. L. *et al.* A new level of conotoxin diversity, a non-native disulfide bond connectivity in alpha-conotoxin AuIB reduces structural definition but increases biological activity. *J. Biol. Chem.* **277**, 48849–48857 (2002).

83. Kuyama, H., Nakajima, C., Nakazawa, T., Nishimura, O. & Tsunasawa, S. A new approach for detecting C-terminal amidation of proteins and peptides by mass spectrometry in conjunction with chemical derivatization. *PROTEOMICS* **9**, 4063–4070 (2009).

84. An, Z., Chen, Y., Koomen, J. M. & Merkler, D. J. A mass spectrometry-based method to screen for α-amidated peptides. *PROTEOMICS* **12**, 173–182 (2012).

85. Jenkins, C. L. & Raines, R. T. Insights on the conformational stability of collagen. *Nat. Prod. Rep.* **19**, 49–59 (2002).

86. Narvaez-Vasquez, J., Pearce, G. & Ryan, C. A. plant cell wall matrix harbors a precursor of defense signaling peptides. *Proc. Natl. Acad. Sci. U. S. A.* **102**, 12974–12977 (2005).

87. Pisarewicz, K., Mora, D., Pflueger, F. C., Fields, G. B. & Marí, F. Polypeptide chains containing D-gamma-hydroxyvaline. *J. Am. Chem. Soc.* **127**, 6207–6215 (2005).

88. Lopez - Vera, E., Walewska, A., Skalicky, J. J., Olivera, B. M. & Bulaj, G. Role of hydroxypyrolines in the in vitro oxidative folding and biological activity of conotoxins. *Biochemistry* **47**, 1741–1751 (2008).

89. Dutertre, S., Nicke, A. & Lewis, R. beta 2 Subunit Contribution to 4/7 alpha -Conotoxin Binding to the Nicotinic Acetylcholine Receptor. *J. Biol. Chem.* **280**, 30460–30468 (2005).

90. Kim, M.-S., Zhong, J. & Pandey, A. Common errors in mass spectrometry-based analysis of post-translational modifications. *PROTEOMICS* **16**, 700–714 (2016).

91. Wolfender, J.-L. *et al.* Identification of tyrosine sulfation in Conus pennaceus conotoxins α-PnIA and α-PnIB: further investigation of labile sulfo- and phosphopeptides by electrospray, matrix-assisted laser desorption/ionization (MALDI) and atmospheric pressure MALDI mass spectrometry. *J. Mass Spectrom.* **34**, 447–454 (1999).

92. Jakubowski, J. A., Kelley, W. P. & Sweedler, J. V. Screening for post-translational modifications in conotoxins using liquid chromatography/mass spectrometry: an important component of conotoxin discovery. *Toxicon* **47**, 688–699 (2006).

93. Soitwisch, J. & Dreisewerd, K. Discrimination of isobaric leucine and isoleucine residues and analysis of post-translational modifications in peptides by MALDI in-source decay mass

spectrometry combined with collisional cooling.(matrix-assisted laser desorption ionization)(Author abstract)(Report). *Anal. Chem.* **82**, 5628–5635 (2010).

94. Langrock, T., Czihal, P. & Hoffmann, R. Amino acid analysis by hydrophilic interaction chromatography coupled on-line to electrospray ionization mass spectrometry. *Amino Acids* **30**, 291–297 (2006).

95. Structure–Activity Studies of Cysteine-Rich α-Conotoxins that Inhibit High-Voltage-Activated Calcium Channels via GABAB Receptor Activation Reveal a Minimal Functional Motif - Carstens - 2016 - Angewandte Chemie International Edition - Wiley Online Library. https://onlinelibrary-wiley-com.eres.library.manoa.hawaii.edu/doi/full/10.1002/anie.201600297.

96. Brady, R. M., Baell, J. B. & Norton, R. S. Strategies for the Development of Conotoxins as New Therapeutic Leads. *Mar. Drugs* **11**, 2293–2313 (2013).

97. Kapono, C. A. *et al.* Conotoxin truncation as a post-translational modification to increase the pharmacological diversity within the milked venom of Conus magus. *Toxicon* **70**, 170–178 (2013).

98. Favreau, P. *et al.* Biochemical Characterization and Nuclear Magnetic Resonance Structure of Novel α-Conotoxins Isolated from the Venom of Conus consors,. *Biochemistry* **38**, 6317–6326 (1999).

99. Leri, A. C. *et al.* Natural organobromine in marine sediments: New evidence of biogeochemical Br cycling. *Glob. Biogeochem. Cycles* **24**, (2010).

100. König, G. M., Wright, A. D., Sticher, O., Angerhofer, C. K. & Pezzuto, J. M. Biological Activities of Selected Marine Natural Products. *Planta Med.* **60**, 532–537 (1994).

101. Bialonska, D. & Zjawiony, J. K. Aplysinopsins - Marine Indole Alkaloids: Chemistry, Bioactivity and Ecological Significance. *Mar. Drugs* **7**, 166–183 (2009).

102. Craig, A. G. *et al.* A Novel Post-translational Modification Involving Bromination of Tryptophan IDENTIFICATION OF THE RESIDUE, L-6-BROMOTRYPTOPHAN, IN PEPTIDES FROM Conus imperialis AND Conus radiatus VENOM. *J. Biol. Chem.* **272**, 4689–4698 (1997).

103. Jimenez, E. C. *et al.* Bromocontryphan: Post-Translational Bromination of Tryptophan †. *Biochemistry* **36**, 989–994 (1997).

104. Aguilar, M. B. *et al.* A novel conotoxin from Conus delessertii with posttranslationally modified lysine residues. *Biochemistry* **44**, 11130–11136 (2005).

105. Kang, J. *et al.* Total chemical synthesis and NMR characterization of the glycopeptide tx5a, a heavily post-translationally modified conotoxin, reveals that the glycan structure is α-d-Gal-(1→3)-α-d-GalNAc. *Eur. J. Biochem.* **271**, 4939–4949 (2004).

106. Craik, D. J. & Adams, D. J. Chemical Modification of Conotoxins to Improve Stability and Activity. *ACS Chem. Biol.* **2**, 457–468 (2007).

107. Bingham, J., A. Jones, R. Lewis, P. Andrews and P. Alewood. Conus venom peptides (conopeptides): inter-species, intra-species and within individual variation revealed by ionspray mass spectrometry. *Biomed. Asp. Mar. Pharmacol.* 13–27 (1996).

108. Teichert, R. W. *et al.* A Uniquely Selective Inhibitor of the Mammalian Fetal Neuromuscular Nicotinic Acetylcholine Receptor. *J. Neurosci.* **25**, 732–736 (2005).

109. Teichert, R. W. *et al.* Definition and characterization of the short alphaA-conotoxins: a single residue determines dissociation kinetics from the fetal muscle nicotinic acetylcholine receptor. *Biochemistry* **45**, 1304–1312 (2006).

110. Bergeron, Z. L. *et al.* A 'conovenomic' analysis of the milked venom from the mollusk-hunting cone snail Conus textile--the pharmacological importance of post-translational modifications. *Peptides* **49**, 145–158 (2013).

111. Hopkins, C. *et al.* A new family of Conus peptides targeted to the nicotinic acetylcholine receptor. *J. Biol. Chem.* **270**, 22361–22367 (1995).

112. Sarin, V. K., Kent, S. B. H., Tam, J. P. & Merrifield, R. B. Quantitative monitoring of solid-phase peptide synthesis by the ninhydrin reaction. *Anal. Biochem.* **117**, 147–157 (1981).

113. Meier, J. & Theakston, R. D. G. Approximate LD 50 determinations of snake venoms using eight to ten experimental animals. *Toxicon* **24**, 395–401 (1986).

114. Peigneur, S. *et al.* Structure-Function Elucidation of a New α-Conotoxin, MilIA, from Conus milneedwardsi. *Mar. Drugs* **17**, 535 (2019).

115. Sugai, C. Characterization of venom from Conus obscurus in search of novel peptide sequences. (2015).

116. Zafaralla, G. C. *et al.* Phylogenetic specificity of cholinergic ligands: .alpha.-conotoxin SI. *Biochemistry* **27**, 7102–7105 (1988).

117. Jacobsen, R. B. *et al.* Critical Residues Influence the Affinity and Selectivity of α-Conotoxin MI for Nicotinic Acetylcholine Receptors †. *Biochemistry* **38**, 13310–13315 (1999).

118. Sines, S. M., Kreienkamp, H.-J., Bren, N., Maeda, R. & Taylor, P. Molecular dissection of subunit interfaces in the acetylcholine receptor: Identification of determinants of α-Conotoxin M1 selectivity. *Neuron* **15**, 205–211 (1995).

119. Groebe, D. R., Dumm, J. M., Levitan, E. S. & Abramson, S. N. alpha-Conotoxins selectively inhibit one of the two acetylcholine binding sites of nicotinic receptors. *Mol. Pharmacol.* **48**, 105–111 (1995).

120. Benie, A. J., Whitford, D., Hargittai, B., Barany, G. & Janes, R. W. Solution structure of α-conotoxin SI. *FEBS Lett.* **476**, 287–295 (2000).

121. Turner, M. W., Marquart, L. A., Phillips, P. D. & McDougal, O. M. Mutagenesis of α-Conotoxins for Enhancing Activity and Selectivity for Nicotinic Acetylcholine Receptors. *Toxins* **11**, 113 (2019).

122. Kasheverov, I. E., Utkin, Y. N. & Tsetlin, V. I. Naturally Occurring and Synthetic Peptides Acting on Nicotinic Acetylcholine Receptors. *Curr. Pharm. Des.* **15**, 2430–2452 (2009).

123. Bren, N. & Sine, S. M. Hydrophobic Pairwise Interactions Stabilize α-Conotoxin MI in the Muscle Acetylcholine Receptor Binding Site. *J. Biol. Chem.* **275**, 12692–12700 (2000).

124. Ning, J. *et al.* Alanine-Scanning Mutagenesis of α-Conotoxin GI Reveals the Residues Crucial for Activity at the Muscle Acetylcholine Receptor. *Mar. Drugs* **16**, (2018).

125. Dutertre, S. & Lewis, R. J. Toxin insights into nicotinic acetylcholine receptors. *Biochem. Pharmacol.* **72**, 661–670 (2006).

126. Groebe, D. R., Gray, W. R. & Abramson, S. N. Determinants Involved in the Affinity of α-Conotoxins GI and SI for the Muscle Subtype of Nicotinic Acetylcholine Receptors †. *Biochemistry* **36**, 6469–6474 (1997).

127. Mordvintsev, D. Y. *et al.* A model for short α-neurotoxin bound to nicotinic acetylcholine receptor from Torpedo Californica. *J. Mol. Neurosci.* **30**, 71–72 (2006).

128. Almquist, R. G. *et al.* Paralytic activity of (des-Glu1)conotoxin GI analogs in the mouse diaphragm. *Int. J. Pept. Protein Res.* **34**, 455–462 (1989).

129. Gray, W. R., Rivier, J. E., Galyean, R., Cruz, L. J. & Olivera, B. M. Conotoxin MI. Disulfide bonding and conformational states. *J. Biol. Chem.* **258**, 12247–12251 (1983).

130. Hashimoto, K. *et al.* Structure-activity relations of conotoxins at the neuromuscular junction. *Eur. J. Pharmacol.* **118**, 351–354 (1985).

131. Guddat, L. W., Martin, J. A., Shan, L., Edmundson, A. B. & Gray, W. R. Three-Dimensional Structure of the α-Conotoxin GI at 1.2 Å Resolution,. *Biochemistry* **35**, 11329–11335 (1996).

132. Liu, L., Chew, G., Hawrot, E., Chi, C. & Wang, C. Two Potent ?3/5 Conotoxins from Piscivorous Conus achatinus. *Acta Biochim. Biophys. Sin.* **39**, 438–444 (2007).

133. Sugiyama, N. *et al.* Residues at the Subunit Interfaces of the Nicotinic Acetylcholine Receptor That Contribute to α-Conotoxin M1 Binding. *Mol. Pharmacol.* **53**, 787–794 (1998).

134. Luo, S. & McIntosh, J. M. Iodo-α-Conotoxin MI Selectively Binds the α/δ Subunit Interface of Muscle Nicotinic Acetylcholine Receptors. *Biochemistry* **43**, 6656–6662 (2004).

135. Espiritu, D. J. D. *et al.* Venomous cone snails: molecular phylogeny and the generation of toxin diversity. *Toxicon* **39**, 1899–1916 (2001).

136. Violette, A. *et al.* Large-scale discovery of conopeptides and conoproteins in the injectable venom of a fish-hunting cone snail using a combined proteomic and transcriptomic approach. *J. Proteomics* **75**, 5215–5225 (2012).

137. López-Vera, E. *et al.* Novel alpha-conotoxins from Conus spurius and the alpha-conotoxin EI share high-affinity potentiation and low-affinity inhibition of nicotinic acetylcholine receptors. *FEBS J.* **274**, 3972–3985 (2007).

138. Armishaw, C. J. & Alewood, P. F. Conotoxins as research tools and drug leads. *Curr. Protein Pept. Sci.* **6**, 221–240 (2005).

139. Quinton, L. *et al.* Identification and functional characterization of a novel α-conotoxin (EIIA) from Conus ermineus. *Anal. Bioanal. Chem.* **405**, 5341–5351 (2013).

140. Echterbille, J. *et al.* Discovery and characterization of EIIB, a new α-conotoxin from Conus ermineus venom by nAChRs affinity capture monitored by MALDI-TOF/TOF mass spectrometry. *Toxicon* **130**, 1–10 (2017).

141. Ning, J. *et al.* Identification of Crucial Residues in α-Conotoxin EI Inhibiting Muscle Nicotinic Acetylcholine Receptor. *Toxins* **11**, 603 (2019).

142. Clark, R. J., Fischer, H., Nevin, S. T., Adams, D. J. & Craik, D. J. The synthesis, structural characterization, and receptor specificity of the alpha-conotoxin Vc1.1. *J. Biol. Chem.* **281**, 23254–23263 (2006).

143. Nicke, A. *et al.* Isolation, structure, and activity of GID, a novel alpha 4/7-conotoxin with an extended N-terminal sequence. *J. Biol. Chem.* **278**, 3137–3144 (2003).

144. Whiteaker, P. *et al.* Discovery, Synthesis, and Structure Activity of a Highly Selective α7 Nicotinic Acetylcholine Receptor Antagonist †. *Biochemistry* **46**, 6628–6638 (2007).

145. Weiss, B., Ebel, R., Elbrächter, M., Kirchner, M. & Proksch, P. Defense metabolites from the marine sponge Verongia aerophoba. *Biochem. Syst. Ecol.* **24**, 1–12 (1996).